2020

The Characterization and Reactivity of Tris(4-methylpyrazolyl)methane and its Tungsten and Molybdenum Metal Complexes

Julia M. Pomeroy
Butler University

BUTLER UNIVERSITY HONORS PROGRAM

Honors Thesis Certification

Please type all information in this section:

Applicant Julia M. Pomeroy
(Name as it is to appear on diploma)

Thesis title The Characterization and Reactivity of Tris(4-methylpyrazolyl)methane and its Tungsten and Molybdenum Metal Complexes

Intended date of commencement December 18, 2020

Read, approved, and signed by:

Thesis adviser(s) _____ Date

_____ Date

Reader(s) _____ Date

_____ Date

Certified by _____ Date
Director, Honors Program

For Honors Program use:

Level of Honors conferred: University _____

Departmental _____

_____

_____

The Characterization and Reactivity of Tris(4-methylpyrazolyl)methane and its Tungsten and Molybdenum Metal Complexes

A Thesis

Presented to the Department of Chemistry and Biochemistry

College of Liberal Arts and Sciences

and

The Honors Program

of

Butler University

In Partial Fulfillment

of the Requirements for Graduation Honors

Julia M. Pomeroy

December 3, 2020

Abstract

The scorpionate ligand tris(pyrazolyl)borate (Tp) has contributed to the understanding of coordination and organometallic chemistry and has proven to be useful in the synthesis of metalloprotein models. Studies focusing on the similar ligand, tris(pyrazolyl)methane (Tpm), have recently been made possible with improved synthetic techniques. Characterization of the Tpm ligand and its metal derivatives, $[TpmW(CO)_3L]^+$ and $[TpmMo(CO)_3L]^+$, unveiled unexpected activity in the ^1H NMR chemical shift of the methane hydrogen after the coordination of a seventh ligand. The more electronegative the seventh ligand was, the more downfield the chemical shift appeared. Various analogs of Tpm have since been synthesized that substitute methyl groups on different positions of the pyrazolyl rings and the effect of these substitutions on the methane hydrogen was examined. This work successfully synthesized an analog of Tpm(4-methyl) and its metal complexes of Tpm(4-methyl)$W(CO)_3$ and Tpm(4-methyl)$Mo(CO)_3$. The reactivity of Tpm(4-methyl)$M(CO)_3$ (M = W or Mo) was observed and FTIR, ^1H NMR, and ^{13}C NMR were used for the characterization of $[Tpm(4\text{-methyl})M(CO)_3L]^+[X]^-$ (L = H, I, or Br; X = counterion). The chemical shift of the methane hydrogen was further examined and determined to follow the same trend seen in the previously reported Tpm metal complexes.

Introduction

A large series of metal complexes containing poly(pyrazolyl)borate or poly(pyrazolyl)methane ligands, particularly tris(pyrazolyl)borate (Tp) or tris(pyrazolyl)methane (Tpm; Figure 1),

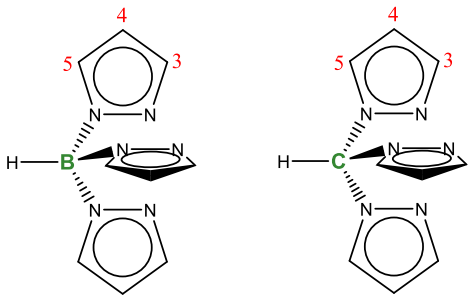

Figure 1: Tris(pyrazolyl)borate (left) and tris(pyrazolyl)methane (right).

were first synthesized by Swiatoslaw Trofimenko.[1] Trofimenko developed and expanded the research on the metal complexes containing tris(pyrazolyl)borate ligands by adding bulky, electron dense substituents onto the pyrazolyl rings, notably at the 3 position. The changes in electronics and sterics altered the overall reactivity of the metal complexes.[2,3] The chemistry of these compounds contributed greatly to our understanding of coordination and organometallic chemistry. For example, some compounds containing Tp have been used as models for metalloproteins.[4,5]

While poly(pyrazolyl)borate metal complexes have been widely studied, less research has been invested in poly(pyrazolyl)methane ligands or their subsequent metal complexes because these ligands had proven to be difficult to synthesize until recently. Research efforts successfully synthesized Tpm in much higher yields than previously reported which have allowed for the larger scale synthesis and examination of the compound and its derivatives.[6,7] Using the new synthetic methods, an analog of Tpm containing methyl groups on the 3 and 5 position on each of the pyrazolyl rings, called Tpm', was efficiently synthesized. The addition of the methyl groups allowed for the examination of the ligand's donor properties compared to the unsubstituted Tpm.[7] Work done in the O'Reilly lab has shown that the additional methyl groups on Tpm' add

electron density to the metal, allowing the metal to more readily act as a Lewis base compared to the metal complexes with the unsubstituted ligand while also increasing the steric demands of the compounds.

The increased research on tris(pyrazolyl)methane ligands and their metal complexes has also led to the observation of intramolecular communication occurring within the metal compounds. When the Tpm ligand was introduced into a metal complex with tungsten or molybdenum and further coordinated with a seventh ligand, H, I, or Br, unexpected changes were observed in the chemical shift of the methane hydrogen. In the uncoordinated Tpm ligand, the methane hydrogen has a chemical shift of 8.73 ppm.[8] This signal appears outside the typical ^{1}H NMR range for alkyl hydrogens but is not surprising due to the three pyrazolyl rings bonded to the methane carbon through a nitrogen atom. The aromaticity of the rings and the electronegativity of the nitrogen atom draw electron density away from the methane hydrogen resulting in a chemical shift seen further downfield. The downfield chemical shift seen in this hydrogen in tris(pyrazolyl)methane is similar to the chemical shift observed for the methane hydrogen of triphenylmethane which also appears outside the expected alkyl range at 5.48 ppm due to the presence of three benzene rings. However, the chemical shift of the methane hydrogen in Tpm was pushed even farther downfield in the Tpm metal complexes that were coordinated to a seventh atom of H, I or Br (Figure 2).

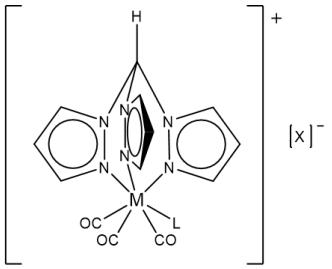

	Hydrogen Chemical Shift	
Ligand (L)	Metal (W)	Metal (Mo)
H	9.57	9.47
I	12.38	11.73
Br	13.09	12.57

J of Organomet Chem. 2007 692, 2887–2896

Figure 2: Charged Tpm metal complex and the chemical shifts of the methane hydrogen with varying ligands. M = W or Mo; X = counterion.

Due to the long distance between the methane hydrogen and the additional ligand, it's unexpected that changes occurring at the seventh coordination site would affect the hydrogen four atoms away. The more electronegative the additional atom was, the more downfield the methane hydrogen signal appeared. This suggests the electronegativity of the added ligand has additive effects with the pyrazolyl rings in withdrawing electron density from the hydrogen. Alternatively, hydrogen bonding could also be contributing to the substantial move downfield. With the multiple electron withdrawing groups drawing electron density away from the methane hydrogen, the CH bond becomes polarized which allows for hydrogen bonding to occur between the counterion present and the methane hydrogen. This communication and potential intermolecular interaction were not observed in the Tp ligands and its metal complexes. In Tp, the hydrogen of interest is connected to a boron atom. Boron nuclei have a spin larger than ½ which leads to the obscuration of the hydrogen signal.[9] The missing hydrogen signal is consistent with the data reported by Trofimenko and others, and, as a result, this activity was only observed recently.[10]

The focus of this research expanded on the knowledge of the observed communication and possible intermolecular interaction. A Tpm ligand analog of Tpm(4-methyl) was synthesized and further introduced into metal complexes via tungsten hexacarbonyl and molybdenum hexacarbonyl, to which additional ligands of varying electronegativity were added. The effect of the methyl group at the 4 position on the pyrazolyl rings was examined with FTIR, ^{1}H NMR, and ^{13}C NMR.

Experimental

General

Reactions were performed under a nitrogen atmosphere using standard Schlenk line techniques. Solvents dichloromethane, hexanes, diethyl ether, and THF were dried using an MBraun Solvent Purification System, and methanol was degassed with nitrogen prior to use. IR spectra were obtained on a Thermo Scientific, Nicolet iS10 FT-IR Spectrometer with ATR capability. ^{1}H NMR and ^{13}C NMR spectra were obtained on a Bruker BioSpin Avance III HD 400 Nanobay System. Reagents not synthesized were purchased from Sigma-Aldrich and Thermo Fisher Scientific. Deuterated solvents were purchased from Cambridge Isotope Laboratories.

Tris(4-methyl-1-pyrazolyl)methane

Fomepizole (2ml, 20mmol) and tetrabutylammonium bromide (0.50g, 1.6mmol) were suspended in DI H_2O (30ml). Sodium carbonate (19.1g, 180mmol) was added gradually to the mixture with continuous stirring. Once the mixture cooled to room temperature, chloroform (15ml, 84mmol) was added and the reaction mixture was allowed to reflux for 3 days. The reaction was cooled to room temperature and filtered via Buchner funnel and washed with diethyl ether. The organic layer was washed with DI H_2O (2x, 30ml), dried with magnesium sulfate, and evaporated. Crude product was recrystallized using hot hexanes. Yield 0.89g (3.5mmol, 43%) white, fluffy solid. ^{1}H NMR (400MHz, dichloromethane-d_2): δ = 8.14 (1H, s), 7.47 (s, 3H), 7.30 (s, 3H), 2.07 (s, 9H).

Tpm(4-methyl)W(CO)$_3$

Tpm(4-methyl) (0.73g, 2.9mmol) and tungsten hexacarbonyl (0.92g, 2.6mmol) were suspended in dimethylformamide (DMF, 40ml) under nitrogen. The reaction mixture was refluxed for 16 hours while under inert atmosphere. The reaction mixture changed from bright orange to brown as the reaction progressed. The mixture was allowed to cool to room temperature and then cooled to 0°C. Cooled methanol (20ml) was added and yellow product precipitated out of solution. The precipitate was filtered via Buchner funnel and washed with methanol. The product was further dried under vacuum and stored under nitrogen at 5°C. Yield 1.16g (2.21mmol, 84%) yellow, fluffy solid.

[Tpm(4-methyl)W(CO)$_3$H]$^+$ [BF$_4$]$^-$

Tpm(4-methyl)W(CO)$_3$ (132mg, 0.251mmol) was put under nitrogen and suspended in dry dichloromethane (15ml). Tetrafluoroboric acid diethyl ether complex (HBF_4, 0.20ml, 1.5mmol) was added, turning the reaction mixture transparent, and dry diethyl ether (50ml) was immediately added, allowing product to precipitate while stirring. Solvent was filtered off via cannula and the remaining product was dried under vacuum. Any remaining HBF_4 was removed by resuspending product in dry diethyl ether and stirring; the ether was removed via cannula and the product was dried under vacuum. Yield was too small to determine. ^{1}H NMR (400MHz, dichloromethane-d_2): δ = 9.19 (s, 1H), 8.07 (s, 3H), 7.92 (s, 3H), 2.02 (s, 9H), -2.66 (s, 1H). ^{13}C NMR (100MHz, dichloromethane-d_2): 214.5 ($^1J_{W\text{-}C}$ = 137 Hz), 149.0, 132.8, 119.9, 75.7, 8.2. IR (dichloromethane): 2020 cm^{-1}, 1932 cm^{-1}, 1911 cm^{-1}.

[Tpm(4-methyl)W(CO)$_3$I]$^+$[I]$^-$

Tpm(4-methyl)W(CO)$_3$ (142mg, 0.271mmol) was put under nitrogen and suspended in dry dichloromethane (15ml). Iodine (0.11g, 0.43mmol) was added and the mixture was allowed to stir until it turned a transparent brown. Dry diethyl ether (50ml) was added to the reaction mixture and allowed to stir until product precipitated. The solvent was removed via cannula and the remaining solid was dried under vacuum. Yield 0.183g (0.24mmol, 86%) rusty, red powder. ^{1}H NMR (400MHz, dichloromethane-d$_2$): δ = 10.02 (s, 1H), 8.64 (s, 3H), 8.40 (s, 3H), 2.22 (s, 9H). ^{13}C NMR (100MHz, dichloromethane-d$_2$): 150.2, 134.3, 120.9, 75.2, 8.6; no signal was observed for CO. IR (dichloromethane): 2035 cm^{-1}, 1959 cm^{-1}, 1926 cm^{-1}.

[Tpm(4-methyl)W(CO)$_3$Br]$^+$[Br]$^-$

Tpm(4-methyl)W(CO)$_3$ (139mg, 0.264mmol) was put under nitrogen and suspended in dry dichloromethane (15ml). Bromine solution (0.5ml, 0.4M, 0.2mmol) was added and the mixture was allowed to stir until it turned a transparent bright orange. The reaction mixture was separated from unreacted starting material and dry diethyl ether (50ml) was added to the reaction mixture to crash product out of solution; no product precipitated. The solvent was removed via evaporation producing a red solid. Yield was too small to determine. ^{1}H NMR (400MHz, dichloromethane-d$_2$): δ = 11.73 (s, 1H), 8.59 (s, 3H), 8.14 (s, 3H), 2.07 (s, 9H). IR (dichloromethane): 2044 cm^{-1}, 1966 cm^{-1}, 1924 cm^{-1}.

Tpm(4-methyl)Mo(CO)$_3$

Tpm(4-methyl) (0.96g, 3.73mmol) and molybdenum hexacarbonyl (1.0g, 3.8mmol) were suspended in DMF (40ml). The reaction mixture was refluxed for 16 hours while under nitrogen. The reaction mixture changed from bright orange to brown as the reaction progressed. The mixture was cooled to room temperature and then put on ice. Cooled methanol (20ml) was added and yellow product precipitated out of solution. The precipitate was filtered via Buchner funnel and washed with methanol. The product was further dried under vacuum and stored under nitrogen at 5°C. Yield 1.4g (3.3mmol, 87%) yellow, fluffy solid.

[Tpm(4-methyl)Mo(CO)$_3$H]$^+$[BF$_4$]$^-$

Tpm(4-methyl)Mo(CO)$_3$ (122mg, 0.280mmol) was put under nitrogen and suspended in dry dichloromethane (15ml) and cooled to -78°C. HBF_4 (0.11ml, 0.84mmol) was added and the reaction mixture was allowed to stir for approximately 30 minutes until it turned transparent. Dry diethyl ether (50ml) was added and the reaction mixture was allowed to stir until product precipitated. The solvent was removed via cannula and the remaining solid was dried under vacuum. Yield 0.055g (0.11mmol, 37%) yellow, flaky solid; decomposed quickly. ^{1}H NMR (400MHz, dichloromethane-d_2): δ = 9.00 (s, 1H), 8.00 (s, 3H), 7.74 (s, 3H), 1.93 (s, 9H), -3.37 (s, 1H). IR (dichloromethane): 2028 cm^{-1}, 1945 cm^{-1}, 1926 cm^{-1}.

[Tpm(4-methyl)Mo(CO)$_3$I]$^+$[I]$^-$

Tpm(4-methyl)Mo(CO)$_3$ (137mg, 0.312mmol) was put under nitrogen and suspended in dry dichloromethane (15ml). Iodine (0.12g, 0.47mmol) was added and the mixture was allowed to stir until it turned a transparent brown. Dry diethyl ether (50ml) was added to the reaction mixture and allowed to stir until product precipitated. The solvent was removed via cannula and the remaining solid was dried under vacuum. Yield 0.132g (0.191mmol, 61%) deep red, powdery solid. ^{1}H NMR (400MHz, dichloromethane-d$_2$): δ = 9.86 (s, 1H), 8.60 (s, 3H), 8.33 (s, 3H), 2.21 (s, 9H). ^{13}C NMR (100MHz, dichloromethane-d$_2$): 149.2, 134.4, 120.3, 74.8, 8.5; no signal was observed for CO. IR (dichloromethane): 2044 cm^{-1}, 1978 cm^{-1}, 1947 cm^{-1}.

[Tpm(4-methyl)Mo(CO)$_3$Br]$^+$[Br]$^-$

Tpm(4-methyl)Mo(CO)$_3$ (145mg, 0.332mmol) was put under nitrogen and suspended in dry dichloromethane (15ml). Bromine (0.03ml, 0.5mmol) was added and the mixture was allowed to stir until it turned a transparent bright orange; solid precipitated out of solution as reaction progressed. Dry diethyl ether (50ml) was added to the reaction mixture and allowed to stir until more product precipitated. The solvent was removed via cannula and the remaining solid was dried under vacuum; obtained solid was not desired product. IR (dichloromethane): 2028 cm^{-1}, 1945 cm^{-1}, 1926 cm^{-1}.

Tris(5-methyl-1-pyrazolyl)methane[11]

Tpm (0.501g, 2.34mmol) was put under nitrogen and suspended in dry THF (5ml). The mixture was allowed to stir at -30°C (acetonitrile and dry ice) for approximately 15

minutes. n-Butyllithium (2.5M in hexanes, 4.8ml, 12mmol) and the reaction was allowed to stir at -30°C for 1 hour; the reaction mixture turned a dark, rusty red brown color. The reaction mixture was then cooled to -78°C (acetone and dry ice) and methyl iodide (0.75ml, 12mmol) was added slowly and dropwise to the reaction, turning it a creamy pale brown. The reaction was allowed to stir at -78°C for 1 hour. The reaction mixture was then warmed to -30°C, and allowed to further warm 0°C. Once at 0°C, the reaction was quenched with methanol (3 drops) and allowed to warm to room temperature. Solvent was removed via evaporation and the remaining solid was dissolved in dichloromethane and washed with DI H_2O (2x, 15ml) and the organic layer was dried with magnesium sulfate and evaporated. Extremely low yield reaction; not enough product to be introduced into metal complex. ^{1}H NMR (400MHz, chloroform-d): δ = 8.31 (s, 1H), 7.51 (d, 1H), 6.14 (d, 1H), 2.09 (s, 3H).

Tris(3-methyl-1-pyrazolyl)methane

3-Methylpyrazole (2ml, 25mmol) and tetrabutylammonium bromide (0.5g, 1.6mmol) were suspended in DI H_2O (30ml). Sodium carbonate (19.0g, 180mmol) was added gradually to the mixture with continuous stirring. Once the mixture cooled to room temperature, chloroform (15ml, 84mmol) was added and the reaction mixture was allowed to reflux for 3 days. The reaction was cooled to room temperature and filtered via Buchner funnel and washed with diethyl ether. The organic layer was washed with DI H_2O (2x, 30ml), dried with magnesium sulfate, and evaporated. Reaction produced a mixture of isomers, Tpm(3-methyl) and Tpm(5-methyl), which were not successfully separated.

I.

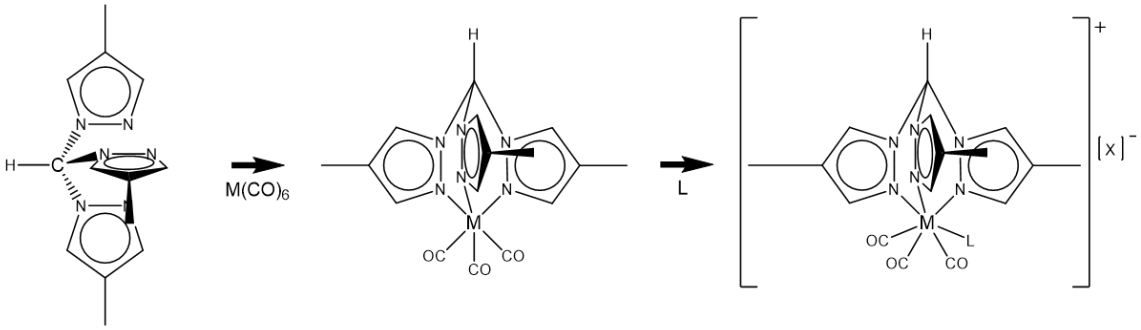

II.

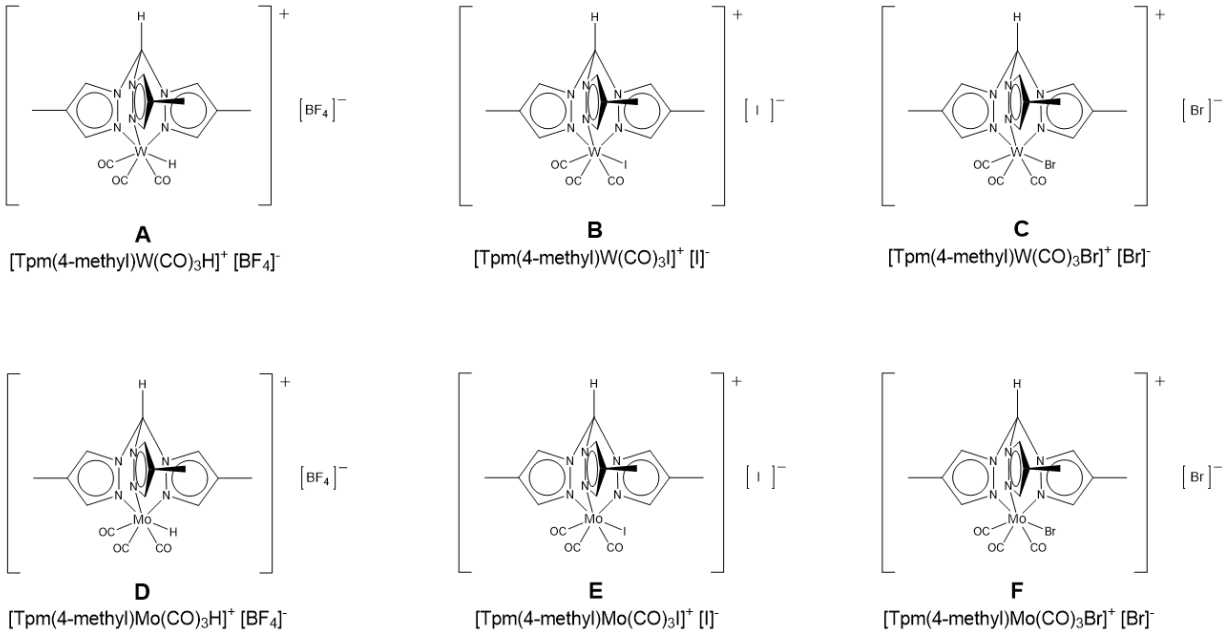

A
[Tpm(4-methyl)W(CO)$_3$H]$^+$ [BF$_4$]$^-$

B
[Tpm(4-methyl)W(CO)$_3$I]$^+$ [I]$^-$

C
[Tpm(4-methyl)W(CO)$_3$Br]$^+$ [Br]$^-$

D
[Tpm(4-methyl)Mo(CO)$_3$H]$^+$ [BF$_4$]$^-$

E
[Tpm(4-methyl)Mo(CO)$_3$I]$^+$ [I]$^-$

F
[Tpm(4-methyl)Mo(CO)$_3$Br]$^+$ [Br]$^-$

Figure 3:
(I) General reaction scheme. M = W or Mo; X = counterion.
(II) Synthesized compounds. Compounds **C** and **F** were not successfully isolated. NMR data for the structures can be seen in Appendix I.

Results and Discussion

Proposed Geometries

Tpm is a tridentate ligand which forms a neutral octahedral compound when introduced into a metal complex via $W(CO)_6$ or $Mo(CO)_6$. The nature of the ligand and the preference of the three remaining CO ligands forces the neutral metal complex into the facial isomerization. When a seventh atom coordinates to the metal complex, it can adopt two different geometries (Figure 4). The 4:3 geometry, also called the piano stool geometry, coordinates the metal-nitrogen bonds on one half of the metal while the other four ligands, three CO groups and one H, I, or Br orient around the bottom half of the metal, similar to the four legs on a piano stool. The 3:3:1 geometry is similar to the octahedral geometry. Again, the tridentate ligand orients around one side of the metal atom while the three CO ligands are also evenly oriented around the other side of the metal. The seventh atom is then bonded to the metal in the center of the three CO ligands.

Crystallography experiments have solved the structure of the neutral Tpm metal complex and its charged complexes with a seventh coordinated atom.[8] It stands to reason that complexes synthesized with Tpm analogs would adopt the same geometries as the parent.

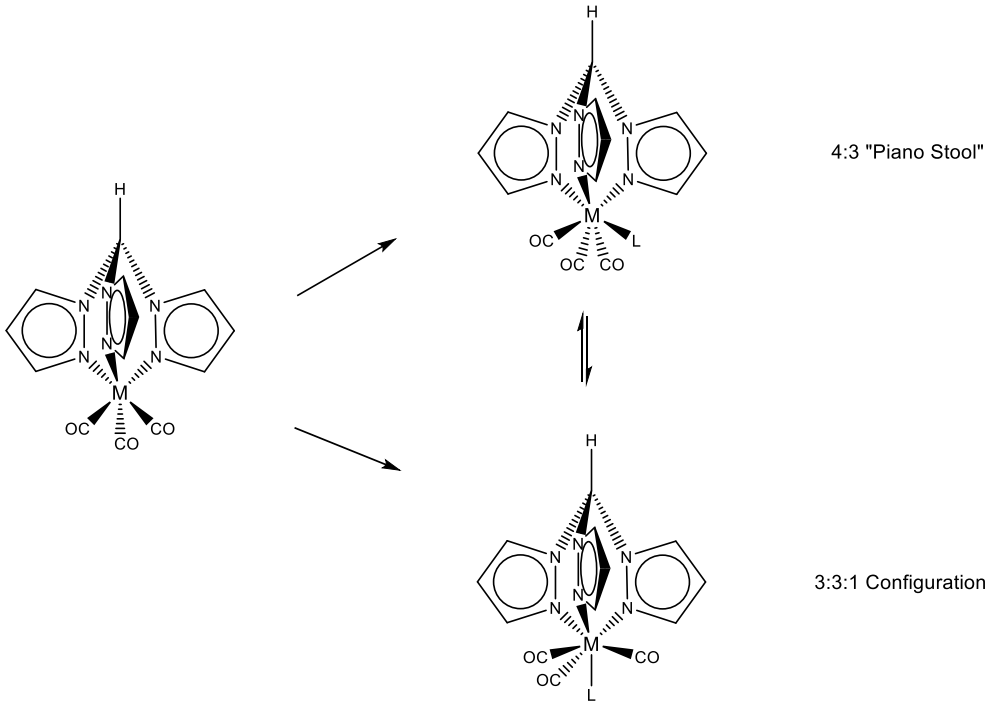

Figure 4: Geometries of the neutral, six-coordinated Tpm and charged, seven-coordinated Tpm metal complexes. M = W or Mo; L = H, I, or Br ligands.

When in solution, the seven-coordinated Tpm complexes fluctuate between the 4:3 and 3:3:1 geometries. The fluxional nature of $[TpmM(CO)_3L]^+$ was also observed in $[TpM(CO)_3L]^+$ and other, similar compounds.[11,13] Based on the ^{13}C NMR obtained, it can be suggested that complexes with the Tpm(4-methyl) ligand also exhibit the fluxional activity seen in Tpm complexes. The ^{13}C NMR for compound **A** shows a peak at 214.5 ppm (Appendix I, pg. 31) which represents the carbon of the CO ligands around the metal. In compounds **B** and **E**, however, there is not a peak that appears in the carbonyl region of the ^{13}C NMR; the CO ligand signals were not captured (Appendix I, pg. 33, 38). Peaks appear in the ^{13}C NMR which correspond to the remaining carbons in both **B** and **E** and IR data confirms the presence of the CO ligands, suggesting the compound is present and has not decarboxylated or decomposed. Instead, the lack of a CO signal in the ^{13}C NMR for **B** and **E** can be explained by the fluctuation of the compounds between the 4:3 and 3:3:1 geometries. When the iodide ligand and the three CO ligands on **B** and **E** are

switching back and forth between the different geometries, it moves at a rate similar to the timescale of the NMR experiment and the NMR is unable to capture the carbons in the CO ligands. The iodide and CO ligands are fluctuating between the 4:3 and 3:3:1 geometries too slowly to produce an accurate average of the geometries. This results in the CO signals being too broad to be observed in the ^{13}C NMR. In contrast, the hydride ligand on **A** is smaller and able to move at a faster rate than the iodide. The fast fluctuation of **A** between the geometries results in sharp, observable signals for the CO ligands and a better approximation of the average of the two geometries. The CO signals for **B** and **E** could possibly be observed if ^{13}C NMR experiments were run at either a warmer temperature or a colder temperature. Running the experiment at warmer temperatures would speed up the fluctuation for the iodide and CO ligands, similar to what's observed for **A**. If the temperature were cooled, the fluctuation of the compound could be slowed drastically and the compound would spend the majority of the experiment in one geometry over the other, which would also allow for sharper signals of the CO ligands as they're essentially staying in the same place. Either way, room temperature is not ideal for ^{13}C NMR experiments on **B** and **E**. ^{13}C NMR spectra were not obtained for compounds **C**, **D**, and **F**.

The ^{13}C NMR spectra obtained for **A** also has satellite signals present on both sides of the tall CO signal. These satellites are indicative of tungsten coupling to the CO carbons. Tungsten-183 nuclei are spin active and has an abundance of approximately 14%. This means that about 14% of the carbon-13 atoms in the CO ligands are bonded to a ^{183}W atom with a spin active nucleus, and the ^{183}W and ^{13}C couple to each other. When this coupling occurs, it results in a doublet that flanks the more prominent CO

signal in the NMR. The satellites represent the 14% of tungsten nuclei that couple to the carbon nuclei, while the prominent middle signal represents the other 86% of carbon nuclei that do not couple to the tungsten they're bonded to.

The synthesized compounds were air sensitive and decomposed when not stored under nitrogen. In general, the complexes containing tungsten were more stable than the molybdenum complexes. Tungsten is larger than molybdenum and thus more able to accommodate the varying electron density of the different ligands. Additionally, the seven-coordinate complexes, for both metals, were more stable when they contained the iodide ligand. This is likely due to iodine being less reactive when compared to other halogens, such as bromine. **C** and **F**, which both have a bromine atom as the seventh coordinated ligand, were unsuccessfully isolated. Compound **F** decarboxylated while in solution; a solid crashed out of solution while the reaction was occurring, and IR spectra showed that over time the presence of the CO ligands in the reaction mixture decreased implying that the solid was the product of CO loss (Appendix I, pg. 39-40). An effort was made to use N-bromosuccinimide as an alternative route to synthesize the bromide metal complexes. IR data showed the metal complex was present while in solution and had IR wavenumbers consistent with previous bromide metal complexes. However, the resulting succinimide ion proved to be an insufficient counterion; when attempting to crash the product out of solution with diethyl ether, the succinimide ion failed to fall out of solution and the obtained solid decomposed. Compound **C**, on the other hand, was able to handle the bromide ligand as evidenced by the CO signals that appeared in the IR (Appendix I, pg. 35) and did not experience decarboxylation. Attempts to crash product out of solution with diethyl ether or hexanes were unsuccessful, and the solvent was removed

via evaporation. Despite the low yield, the ^{1}H NMR showed that **C** was successfully synthesized (Appendix I, pg. 34); future isolation will need to be altered to increase yield. **A** and **D** contained the hydride ligand and decomposed quickly. The tungsten hydride was stable enough to obtain a ^{13}C NMR spectra while the molybdenum hydride appeared to start decomposing immediately. Evidence of the molybdenum hydride's decomposition can be seen in its ^{1}H NMR (Appendix I, pg. 36), and the collected solid, which was initially yellow, turned black and decomposed while under nitrogen within 30 minutes of synthesis. It's likely that HBF_4 was present in the collected product and contributed to the fast decomposition of the compound. In future experiments, this could potentially be avoided by adding a "proton sponge" to the reaction mixture before product isolation to prevent decomposition.

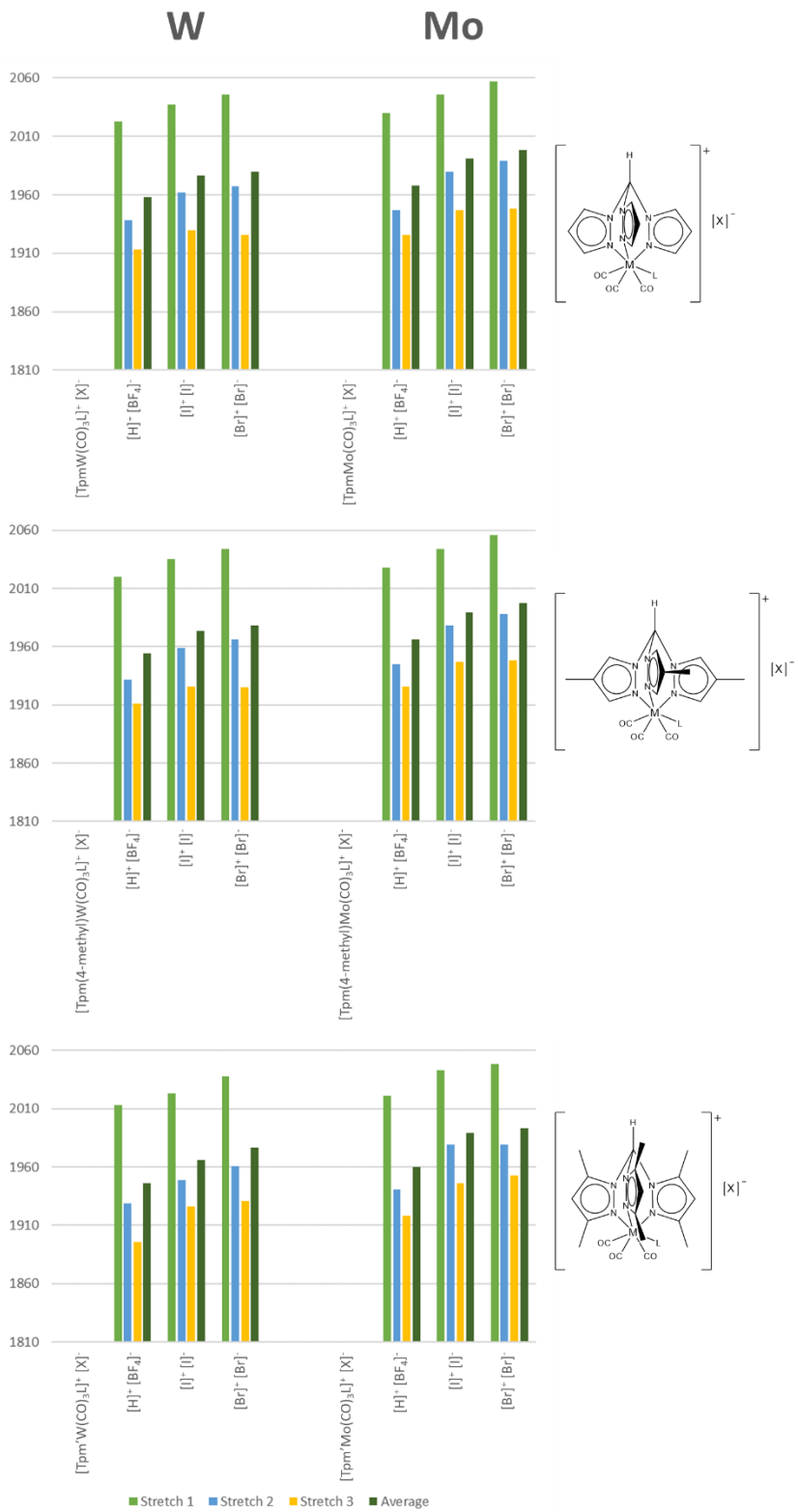

Figure 5: CO Infrared Stretches of Coordination Compounds. M = W or Mo; X = counterion. IR wavenumbers are reported in Appendix I.

FTIR

Due to the presence of the three CO ligands, which are pi acids, all of the synthesized compounds experienced pi backbonding (Figure 6). In the examined complexes, the metal and CO ligand form a sigma bond; the electron density in the sigma bond is donated from the carbon to the metal. The metal's t_{2g} d orbital is symmetric to the empty carbon antibonding pi orbital, and electron density in the metal's t_{2g} orbital can be pushed back toward the ligand into its antibonding orbital. Backbonding contributes to the stabilization of the compounds because it allows for the electron density of the metal to be spread out which lowers the energy of the metal's d orbital. When backbonding occurs, it can be monitored using FTIR. CO has a bond length of 112.8 pm and a stretching frequency in the FTIR of 2135 cm^{-1}. Changes in bond length will impact the energy required to stretch the CO bond.

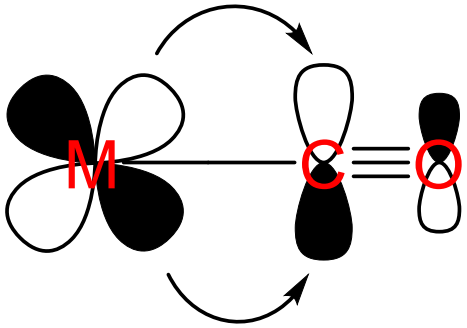

Figure 6: pi Backbonding. Excess electron density from the metal d orbital is pushed back to the carbon antibonding pi orbital in CO.

While IR values are given as a wavenumber, the inverse of the wavelength is in centimeters; the energy needed to stretch a bond is explained using Plank's quation:

$$E = hv = \frac{hc}{\lambda} = hc\bar{v}$$

$$\bar{v} = \frac{1}{\lambda}$$

h = Plank's constant
v = velocity
c = speed of light
λ = wavelength
$\bar{v}$ = wavenumber

The length of CO bonds can be altered due to backbonding. When backbonding occurs, electron density is being pushed into the CO antibonding pi orbital which weakens and elongates the CO bond to longer than 112.8 ppm and lowers the energy stretch. As the degree of backbonding increases, more electron density is being donated to the CO ligands, resulting in a lower energy stretch and wavenumbers observed in the IR.

The synthesized compounds experienced backbonding, and the identity of the ligands and the metal in the different complexes resulted in alterations of the CO ligands' bond strengths. The IR stretching frequencies (Figure 5; Appendix I pg. 43) of the various metal complexes followed the expected trends based on pi backbonding. Tungsten is a larger, more electron dense atom than molybdenum, so it was expected that complexes containing tungsten would exhibit lower number in the IR compared to their molybdenum counterparts. This trend was observed (Figure 5). Additionally, the Tpm parent ligand is the least electron dense of the analyzed ligands; Tpm(4-methyl) has one additional methyl group on each pyrazolyl, and Tpm' has two additional methyl groups subsitituted on the pyrazolyl rings making Tpm' the most electron dense ligand. With these three ligands, it was expected that complexes with Tpm would experience the least amount of backbonding and Tpm' complexes would experience the most, with Tpm(4-methyl) complexes experiencing a degree of backbonding that was inbetween that seen in Tpm and Tpm'. In short, the resulting CO bond strengths for the ligands was expected to be Tpm > Tpm(4-methyl) > Tpm'. This general trend was observed; however, metal complexes that had the Tpm(4-methyl) ligand experienced only a slight shift in CO stretching frequency when compared to their Tpm counterparts. This suggests that

adding a single methyl group to each pyrazolyl ring does not add enough electron density toward the metal to significantly alter the backbonding occuring.

The degree of backbonding was further altered with the coordination of a seventh atom of either H, I, or Br. Like the CO ligands, H, I, and Br ligands can accept electron density from the metal. When an H, I, or Br is bonded alongside the three CO ligands, they will further reshape the electron density at the metal center with the three CO ligands. These ligands are electronegaitve atoms and their corresponding electronegativity affected how much of the electron denisty of the metal is pushed toward the H, I, or Br. This results in the CO ligands getting a smaller share of the backbonding occuring and stronger CO bond lengths are observed when compared to the neutral octahedral complexes. The bromide ligand is the most electronegitive of those studied and is able to pull more electron density from the metal than H or I. As such, metal complexes containing the bromide ligand exhibited higher IR stretching frequencies due to the stronger CO bond lengths resulting from less backbonding occuring with the CO ligands. The opposite can be said of metal complexes containing the hydride ligand, which is the least electronegitive and will not impact the electron density as much as I or Br. More backbonding was observed in the CO ligands, and, as expected, the hydride complexes exhibited lower IR stretching frequencies compared to the iodide and bromide complexes.

Reactivity

In addition to the identity of the metal and ligands affecting the backbonding into CO ligands, they also affected the complex's reactivity, particularly in the metal's ability to act as a Lewis base. Tungsten, which is electron dense, acts as a better Lewis base when compared to molybdenum. As a result, tungsten complexes tended to react faster than molybdenum complexes and the tungsten complexes had less difficulty coordinating a seventh ligand. With the addition of the ligands, particulary electron dense ligands, both metals are able to act as Lewis bases. Whether a reaction was done was determined by the transition of the reaction mixture from a murky solution to a transparent solution. The $TpmM(CO)_3$ starting material, and its Tpm analog variants, is insoluble in the dichloromethane solvent while the seven-coordinated complexes are soluble in dichloromethane. Complexes containing molybdenum and either Tpm or Tpm(4-methyl) reacted the slowest and these reactions often had to be stirred for thirty minutes or longer. However, Tpm', with its methyl substitutions on the 3, 5 positions, provided enough electron density for its molybdenum complex and extended times were not needed for reactions using $Tpm'Mo(CO)_3$ as the Lewis base. Meanwhile, tungsten complexes containing Tpm, Tpm', or Tpm(4-methyl) reacted quickly and reaction mixtures typically turned transparent with less than five minutes of stiring. The quickness of the reactions can be related to the electron density of the metals which can be indirectly observed through backbonding toward the CO ligands. Overall, the metal complexes followed the expected trend that the more electron density being pushed toward the metal, the more efficient the metal would be as a Lewis base.

It's also possible that the position of the methyl groups are affecting the reactivity of the complexes as well. Alkorta, et al. suggests that the electronics are different among of the 3, 4, and 5 positions on the pyrazolyl rings.[13] So, metal complexes containing Tpm' or Tpm(4-methyl) experience different electronics that could alter their reactivity in addition to the amount of electron density being added by the different ligands. This could be further explored by synthesizing the Tpm analogs of Tpm(3-methyl) and Tpm(5-methyl) to determine how the electronics of singular methyl groups at each position affects metal complexes when compared to the Tpm(4-methyl) ligand.

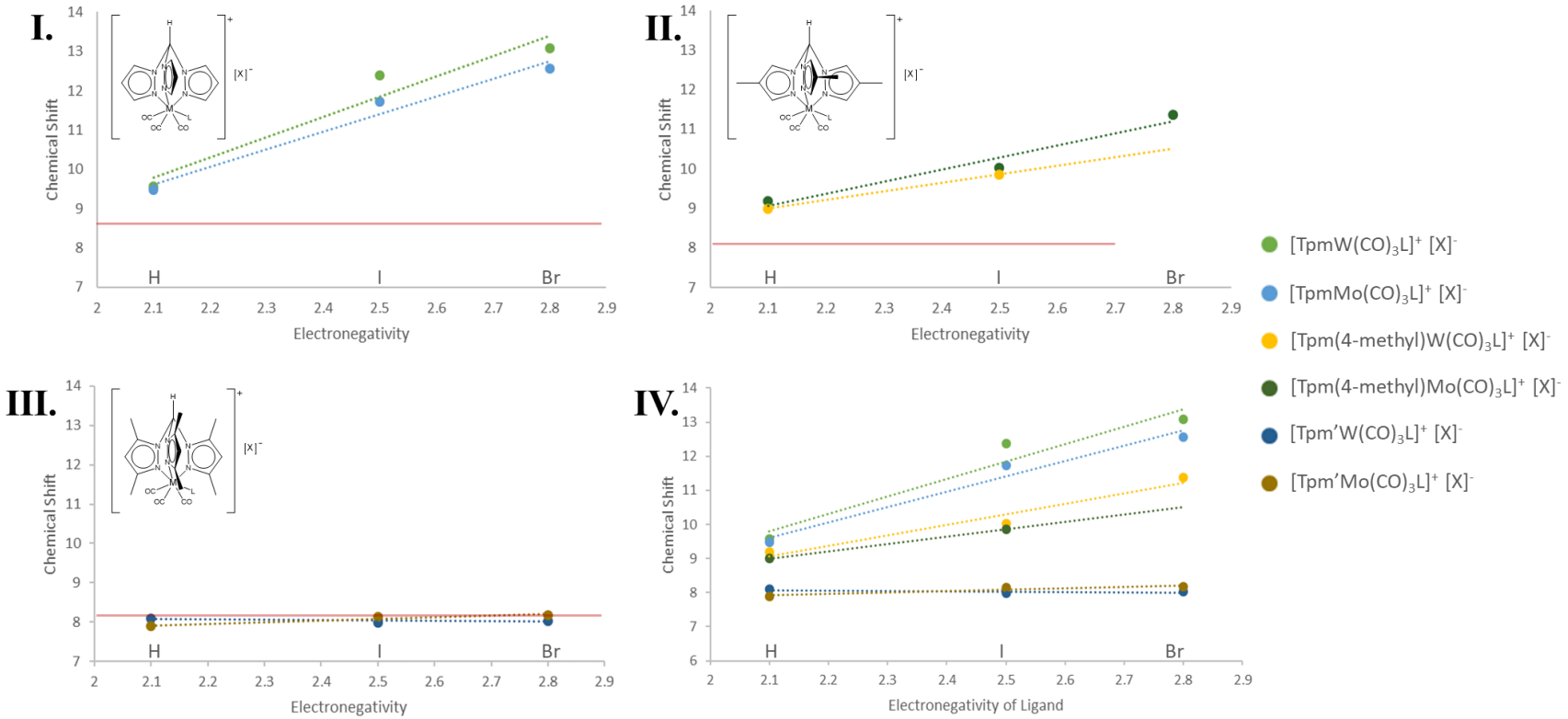

Figure 7: Change in Chemical Shift of Methane Hydrogen in Various Seven-Coordinated Metal Complexes. (I) $TpmM(CO)_3$ **(II)** Tpm(4-methyl)$M(CO)_3$ **(III)** Tpm'$M(CO)_3$ **(IV)** All of the chemical shifts together. The red line indicates the chemical shift of the methane hydrogen in the corresponding non-coordinated ligand. ^{1}H NMR data for Tpm(4-methyl) metal complexes can be seen in Appendix I.

^{1}H NMR

Of particular interest for this work was the chemical shift in the ^{1}H NMR. On the uncoordinated Tpm(4-methyl) ligand, the hydrogen had a chemical shift at 8.14 ppm. As seen with the Tpm ligand (Figure 7, I), when the Tpm(4-methyl) ligand was introduced into a seven-coordinated metal complex, the chemical shift of the methane hydrogen changed drastically based on the identity of the seventh-coordinated atom (Figure 7, II). The more electronegative the seventh ligand was, the more downfield the chemical shift appeared, presumably due to the electron density being pulled away from the methane hydrogen by the added H, I, or Br ligand. For the Tpm' ligand, however, the chemical shift of the methane hydrogen didn't change according to the expected trend (Figure 7, III). This suggests that it's not just the identity of the seventh-coordinated ligand altering the chemical shift of the methane hydrogen. The Tpm' methane hydrogen deviating from the expected trend in chemical shift is likely due to the methyl groups at position 5 on the ligand, but it may be a steric or electronic effect.

As discussed earlier, the methane CH bond can become polarized when enough electron density is pulled away from the hydrogen. This allows for the hydrogen to be accessible for hydrogen bonding. Each of the seven-coordinated metal complexes synthesized are cationic and are stabilized by the presence of an anionic counterion. The counterions are free to move within the solution and can hydrogen bond to the methane hydrogen when it becomes polarized. This intermolecular interaction can contribute to the shift in chemical shift seen in Tpm and Tpm(4-methyl) metal complexes as the counterions can also pull electron density from the methane hydrogen. Compared to the distance of between the methane hydrogen and the seventh-coordinated ligand, the

proximity of the counterion provides a more logical explanation for the drastic change seen in chemical shift. Unlike Tpm and Tpm(4-methyl), Tpm' has a methyl group substituted at the five position on each of the pyrazolyl rings. The methyl groups at this position adds steric clash around the methane hydrogen that could hinder a counterion's attempts to hydrogen bond to the polarized hydrogen. The blocking of this hydrogen bond would result in no drastic changes in the chemical shift of the methane hydrogen, which was observed for the Tpm' metal complexes (Figure 7, III).

Further examination would be needed to verify if hydrogen bonding was occurring. It's possible to synthesis a Tpm(5-methyl) ligand, but the procedure described produced yields too small to introduce the ligand into metal complexes. A ligand containing only one methyl group at position 5 on each of the pyrazolyl rings would add evidence for whether the change in chemical shift is due to hydrogen bonding or the electronegativity of the seventh-coordinated ligand. Additionally, a Tpm(5-methyl) ligand would theoretically donate a similar amount of electron density as the Tpm(4-methyl) ligand and it's been observed that Tpm(4-methyl) metal complexes follow the expected trend in chemical shift changes. If Tpm(5-methyl) produced results similar to Tpm' it could be concluded that the change in chemical shift is hindered by steric clash and not the additional electron density Tpm' pushes into the pyrazolyl rings. If hydrogen bonding is not occurring, it'd be expected that the Tpm(5-methyl) ligand would follow the same trend seen in Tpm(4-methyl) metal complexes.

Conclusion

In this work, changes in the methane hydrogen's chemical shift of Tpm(4-methyl) metal complexes were determined to follow a similar trend to that observed in Tpm metal complexes. When compared to the chemical shifts obtained for Tpm' metal complexes, however, data suggests that the change in chemical shift is due to hydrogen bonding occurring between counter ions and the methane hydrogen. Future experiments would need to successfully synthesize a Tpm(5-methyl) ligand in high yields in order to examine trends seen in Tpm(5-methyl) metal complexes and compare to what was observed for the Tpm' and Tpm(4-methyl) ligands. Crystallography experiments could also provide more information as to whether hydrogen bonding is occurring.

Literature Cited

1. Trofimenko, Swiatoslav. Geminal Poly(1-Pyrazolyl)Alkanes and Their Coordination Chemistry. *J. Am. Chem. Soc.* 1970, *92* (17), 5118–5126.
2. Trofimenko, S.; Rheingold, A. L.; Liable Sands, L. M. Coordination Chemistry of Novel Scorpionate Ligands Based on 3-Cyclohexylpyrazole and 3-Cyclohexyl-4-Bromopyrazole. *Inorg. Chem.* 2002, *41* (7), 1889–1896.
3. Trofimenko, S. Recent Advances in Poly(Pyrazolyl)Borate (Scorpionate) Chemistry. *Chem. Rev.* 1993, *93* (3), 943–980.
4. Jacobsen, F. E.; Lewis, J. A.; Heroux, K. J.; Cohen, S. M. Characterization and Evaluation of Pyrone and Tropolone Chelators for Use in Metalloprotein Inhibitors. *Inorganica Chimica Acta* 2007, *360* (1), 264–272.
5. Puerta, D. T.; Schames, J. R.; Henchman, R. H.; McCammon, J. A.; Cohen, S. M. From Model Complexes to Metalloprotein Inhibition: A Synergistic Approach to Structure-Based Drug Discovery. *Angew. Chem.* 2003, 3.
6. Bigmore, H. R.; Lawrence, S. C.; Mountford, P.; Tredget, C. S. Coordination, Organometallic and Related Chemistry of Tris(Pyrazolyl)Methane Ligands. *Dalton Trans.* 2005, 17.
7. Reger, D. L.; Grattan, T. C.; Brown, K. J.; Little, C. A.; Lamba, J. J. S.; Rheingold, A. L.; Sommer, R. D. Syntheses of Tris(Pyrazolyl)Methane Ligands and {[Tris(Pyrazolyl)Methane]Mn(CO)3}SO3CF3 Complexes: Comparison of Ligand Donor Properties. *Journal of Organometallic Chemistry* 2000, 9.
8. Dilsky, S. Molybdenum and Tungsten Complexes of the Neutral Tripod Ligands HC(Pz)3 and MeC(CH2PPh2)3. *Journal of Organometallic Chemistry* 2007, *692* (14), 2887–2896.
9. Reed, D. The Role of NMR in Boron Chemistry. *Chem. Soc. Rev.* 1993, *22* (2), 109.
10. Curtis, M. D.; Shiu, K. B. Synthesis, Structure, and Fluxional Behavior of 7-Coordinate Complexes: TpMo(CO)3X (X = H, Br, I; Tp = Hydridotripyrazolylborato). 6.
11. Goodman, M. A.; Nazarenko, A. Y.; Casavant, B. J.; Li, Z.; Brennessel, W. W.; DeMarco, M. J.; Long, G.; Goodman, M. S. Tris(5-Methylpyrazolyl)Methane: Synthesis and Properties of Its Iron(II) Complex. *Inorg. Chem.* 2012, *51* (2), 1084–1093.
12. Baker, M. V.; North, M. R.; Skelton, B. W.; White, A. H. Oxidations of (R_3 Tach)$M(CO)_3$ Complexes [M = Cr, Mo, W; R_3 Tach = 1,3,5-Trialkyl-1,3,5-Triazacyclohexane (R = *t*-Bu, Bn)]. Crystal Structures of (*t*-Bu_3 Tach)$MO_3 \cdot 15H_2O$ (M = Mo, W). *Inorg. Chem.* 1999, *38* (20), 4515–4521.
13. Alkorta, I.; Claramunt, R. M.; Díez-Barra, E.; Elguero, J.; López, C. The Organic Chemistry of Poly(1H-Pyrazol-1-Yl)Methanes. *Coordination Chemistry Reviews* 2017, 31.

Appendix I

Table 1: Table of Abbreviations

Abbreviation	Full Term
Tp	Tris(pyrazolyl)borate
Tpm	Tris(pyrazolyl)methane
Tpm’	Tris(3,5-dimethylpyrazole)methane
Tpm(4-methyl)	Tris(4-methylpyrazole)methane
Tpm(3-methyl)	Tris(3-methylpyrazole)methane
Tpm(5-methyl)	Tris(5-dimethylpyrazole)methane
$TpmW(CO)_3$	Tricarbonyltris(pyrazolyl)methanetungsten (0)
$TpmMo(CO)_3$	Tricarbonyltris(pyrazolyl)methanemolybdenum(0)
$Tpm'W(CO)_3$	Tricarbonyltris(3,5-dimethylpyrazolyl)methanetungsten(0)
$Tpm'Mo(CO)_3$	Tricarbonyltris(3,5-dimethylpyrazolyl)methanemolybdenum(0)
$Tpm(4\text{-methyl})W(CO)_3$	Tricarbonyltris(4-methylpyrazolyl)methanetungsten(0)
$Tpm(4\text{-methyl})Mo(CO)_3$	Tricarbonyltris(4-methylpyrazolyl)methanemolybdenum(0)
M	Metal (W or Mo)
L	Ligand (H, I or Br)
W	Tungsten
Mo	Molybdenum
H	Hydride Ligand
I	Iodide Ligand
Br	Bromide Ligand
CO	Carbon monoxide carbonyl ligand
$W(CO)_6$	Tungsten hexacarbonyl
$Mo(CO)_6$	Molybdenum hexacarbonyl
HBF_4	Tetrafluoroboric acid diethyl ether complex
THF	Tetrahydrofuran
DMF	Dimethylformamide
DI H_2O	Deionized water
FTIR (IR)	Fourier transform infrared
^{1}H NMR	Proton nuclear magnetic resonance
^{13}C NMR	Carbon nuclear magnetic resonance
ppm	Parts per million
pm	Picometers
cm^{-1}	Wavenumber

Tris(4-methyl-1-pyrazolyl)methane: $HC(C_4H_5N_2)_3$

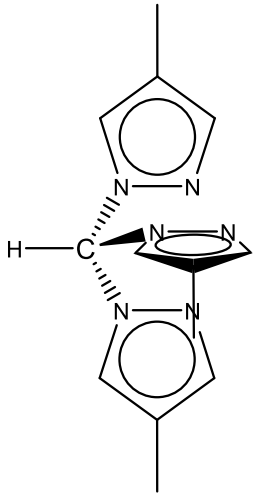

^{1}H NMR: chloroform-d

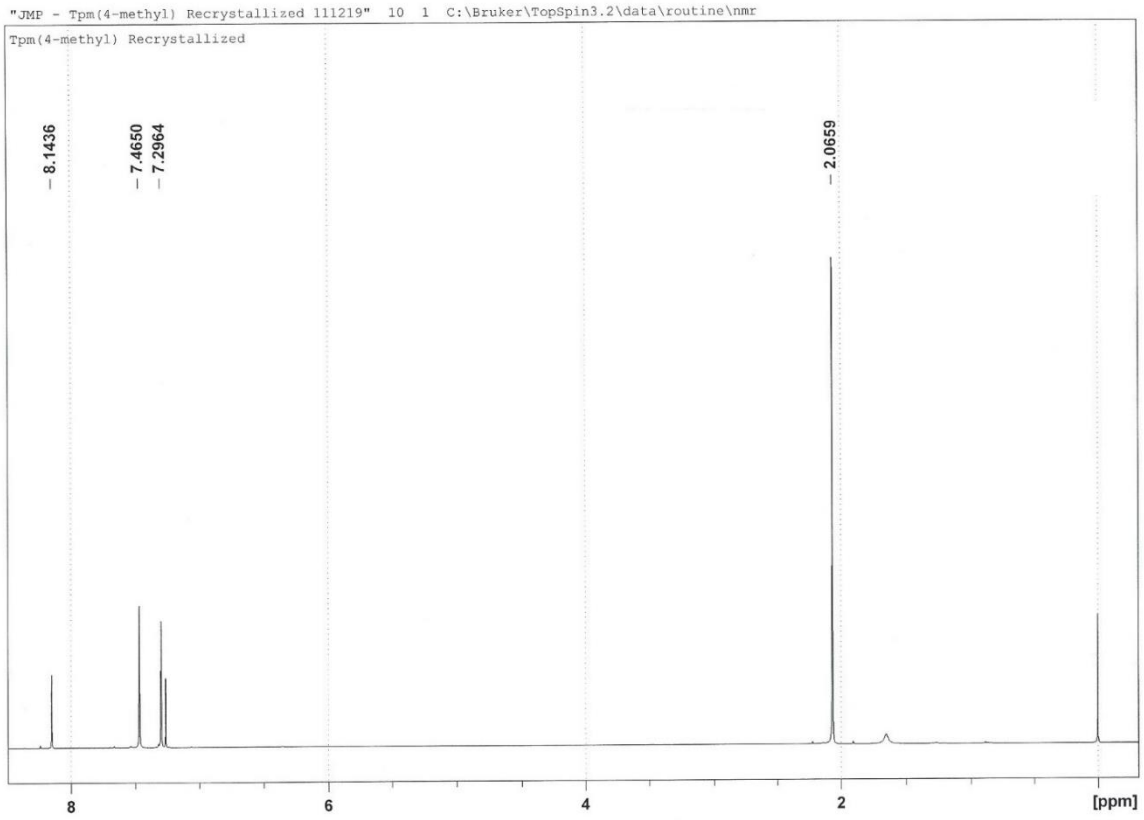

[Tpm(4-methyl)W(CO)$_3$H]$^+$ [BF$_4$]$^-$: [HC(C$_4$H$_5$N$_2$)$_3$W(CO)$_3$H]$^+$[BF$_4$]$^-$

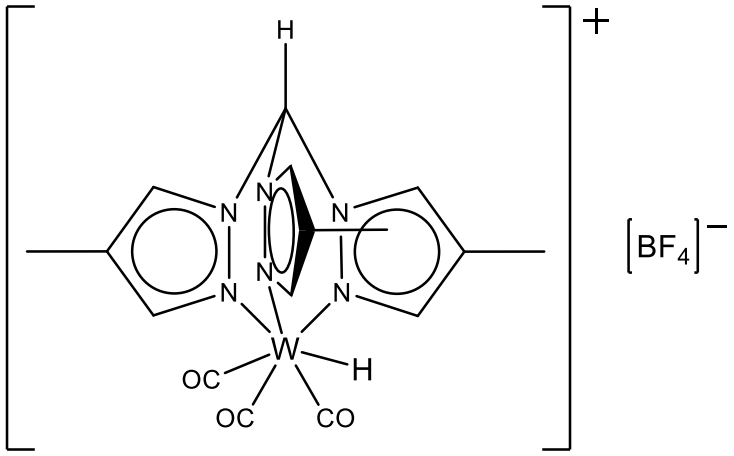

^{1}H NMR: dichloromethane-d$_2$

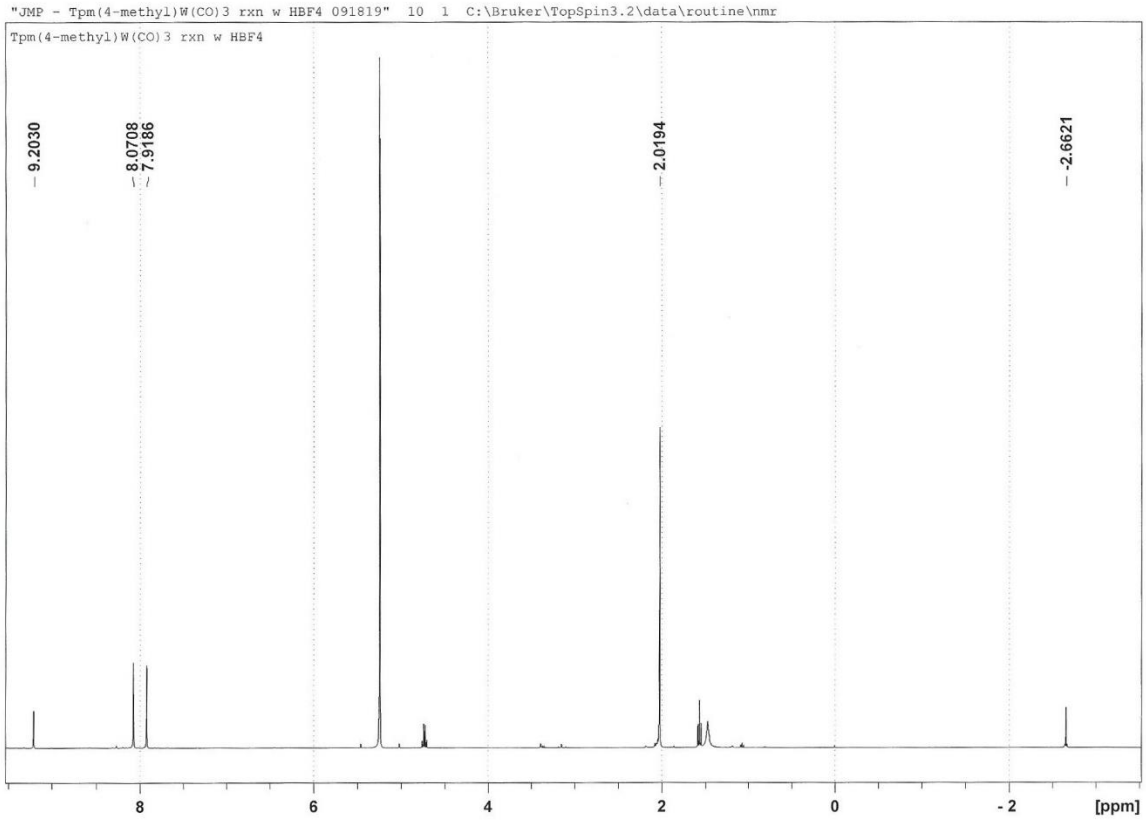

^{13}C NMR: dichloromethane-d_2

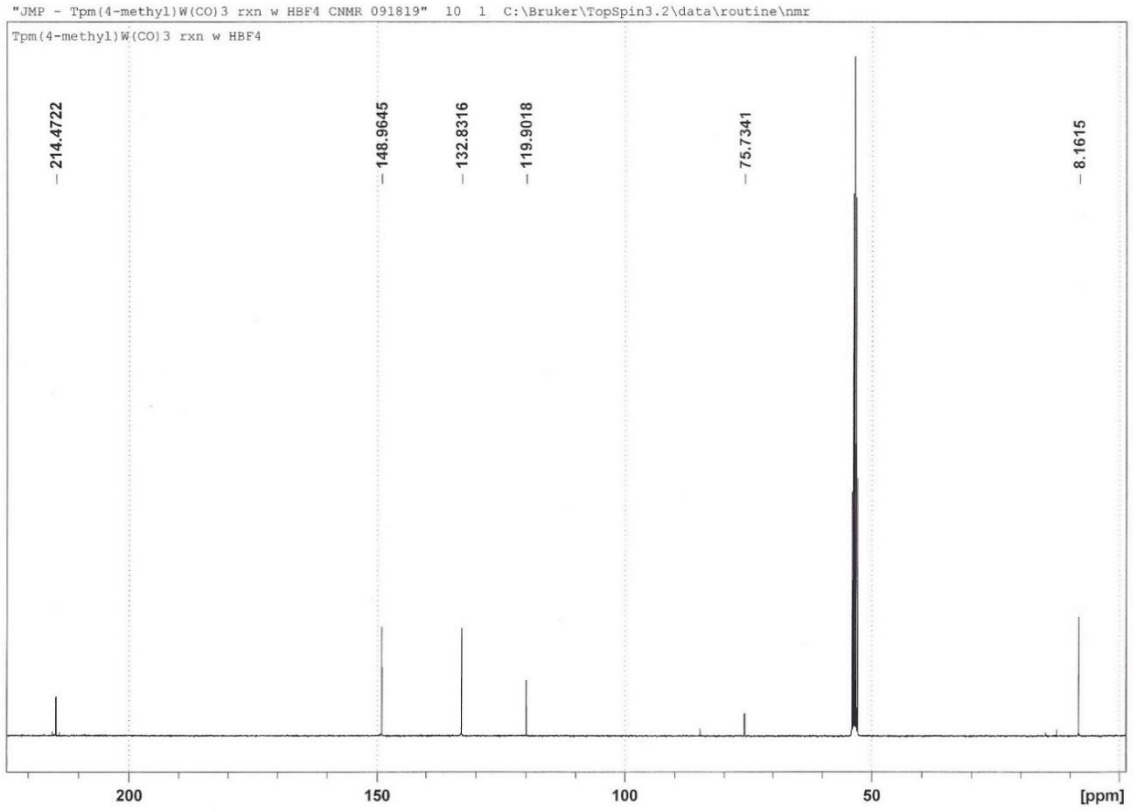

[Tpm(4-methyl)W(CO)$_3$I]$^+$ [I]$^-$: [HC(C$_4$H$_5$N$_2$)$_3$W(CO)$_3$I]$^+$[I]$^-$

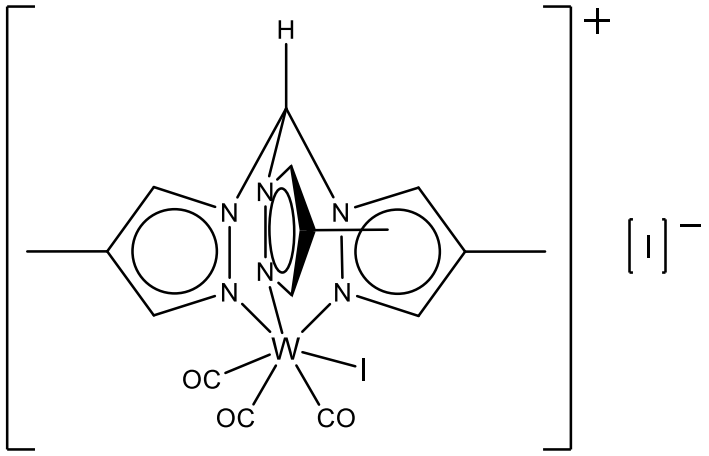

^{1}H NMR: dichloromethane-d$_2$

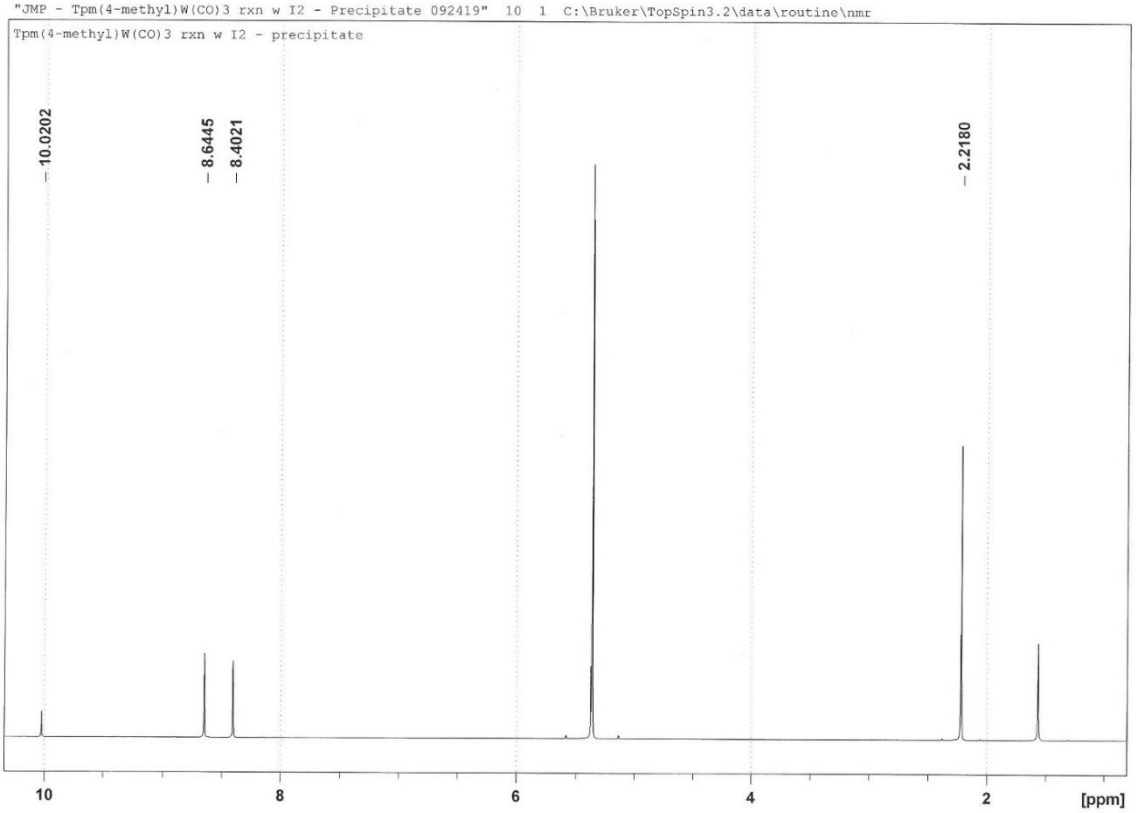

^{13}C NMR: dichloromethane-d_2

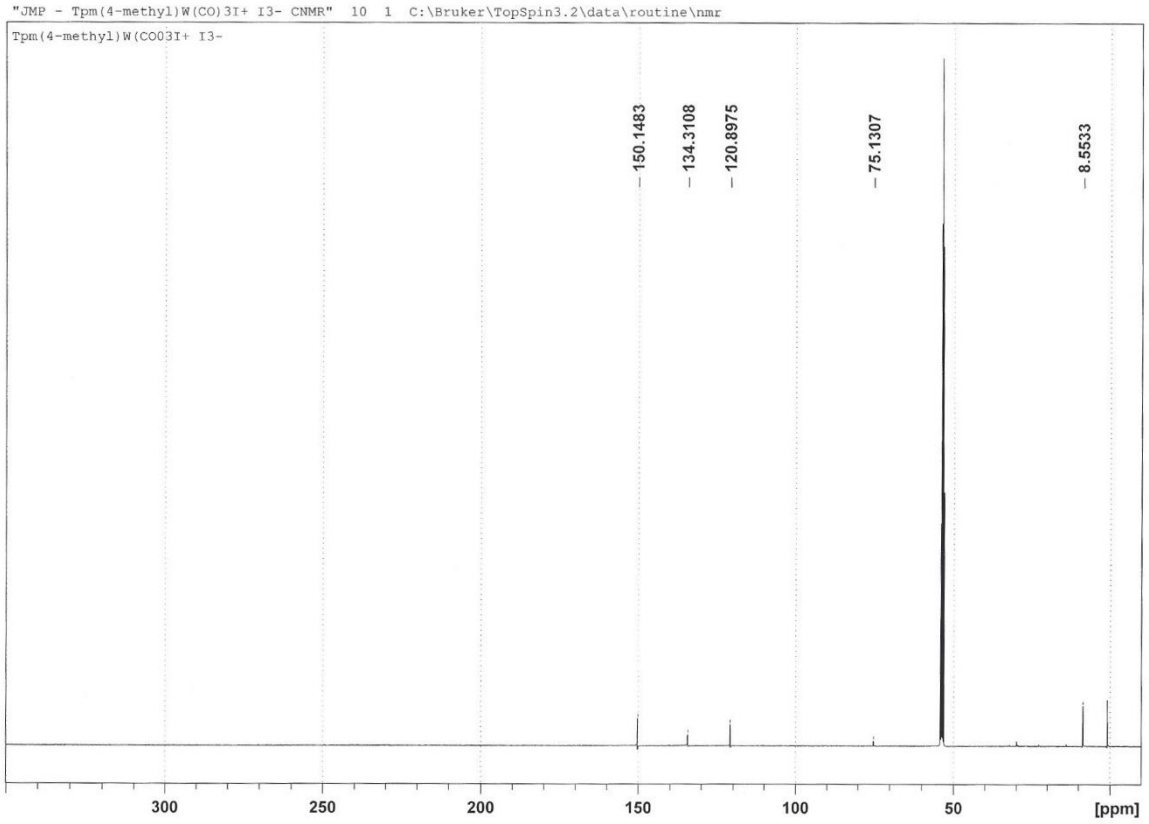

[Tpm(4-methyl)W(CO)$_3$Br]$^+$ [Br]$^-$: [HC(C$_4$H$_5$N$_2$)$_3$W(CO)$_3$Br]$^+$[Br]$^-$

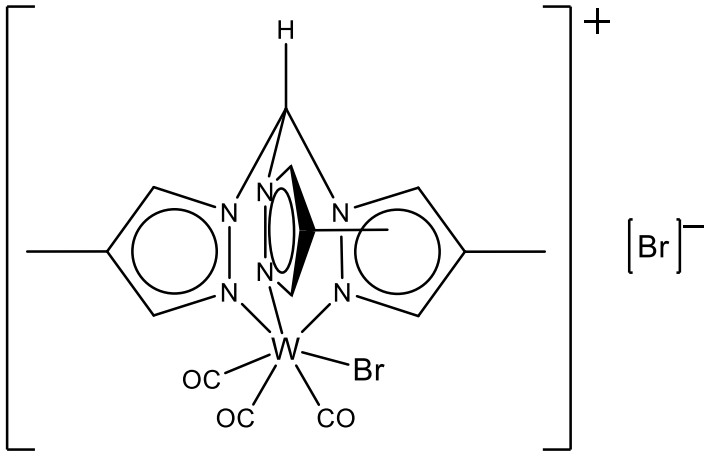

^{1}H NMR: dichloromethane-d$_2$

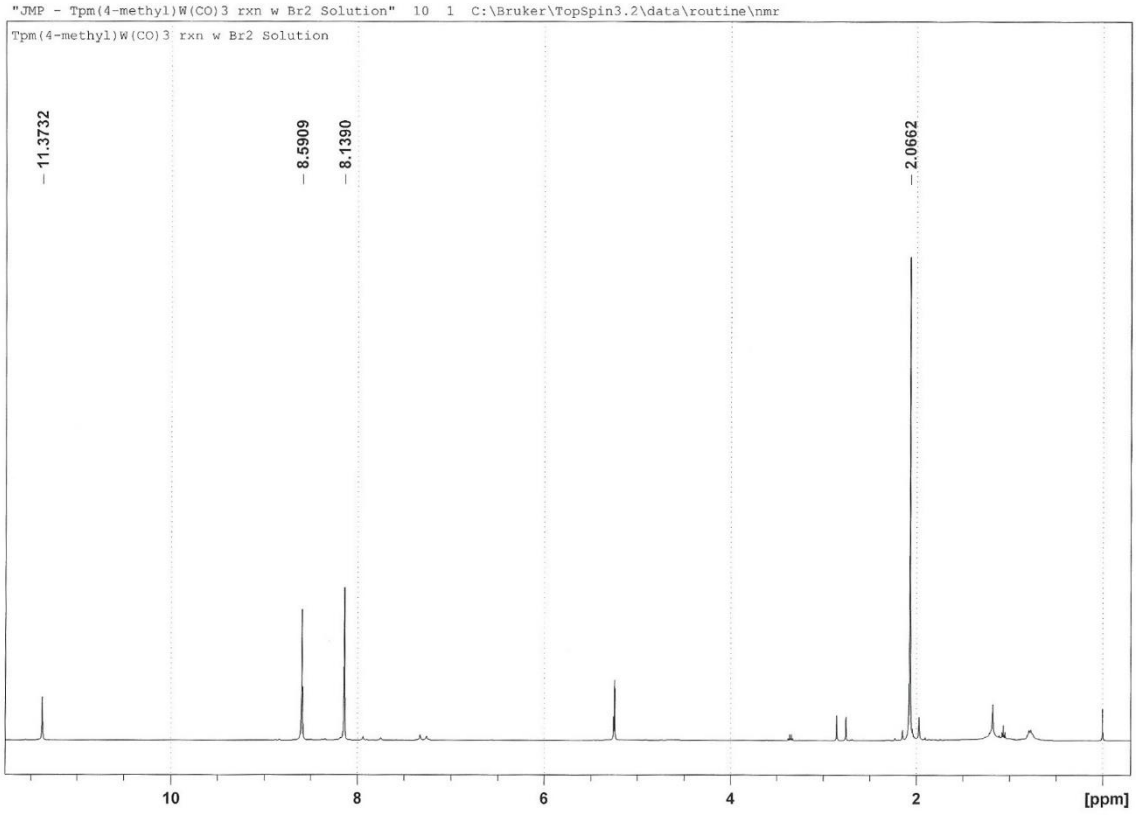

IR: dichloromethane

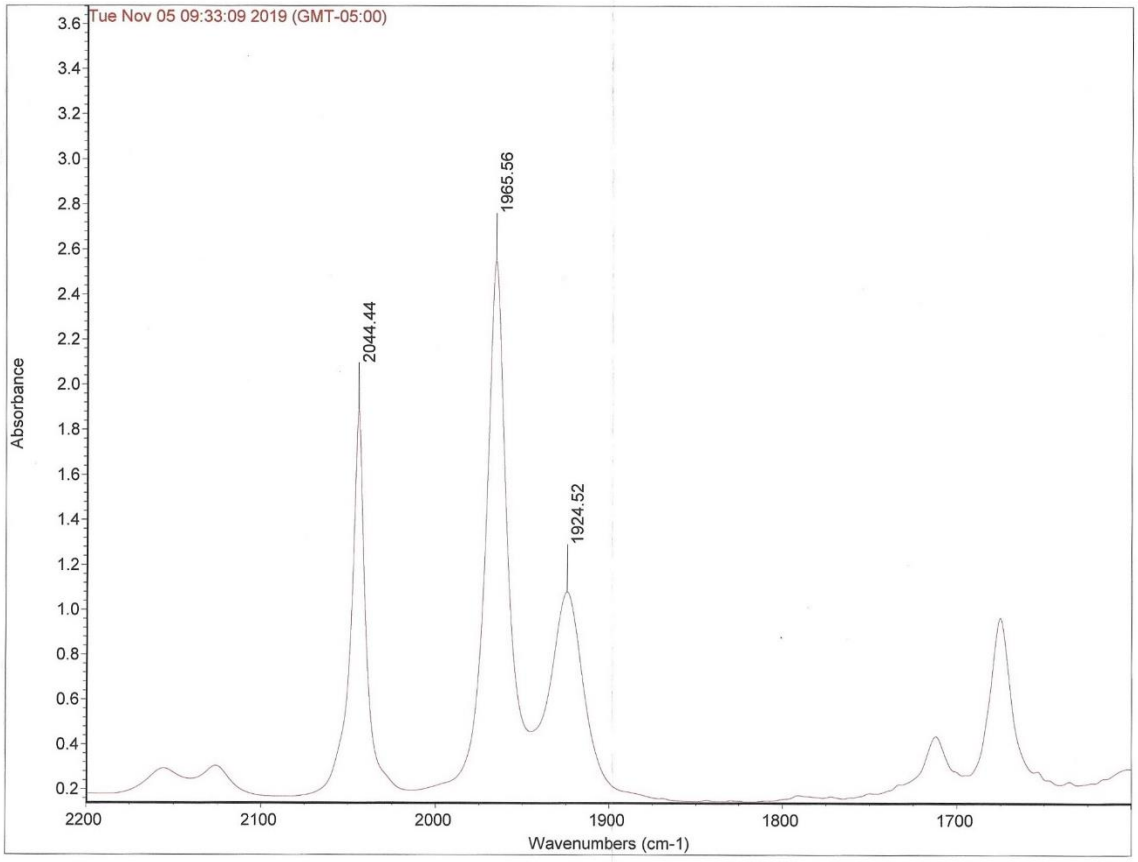

[Tpm(4-methyl)Mo(CO)$_3$H]$^+$ [BF$_4$]$^-$: [HC(C$_4$H$_5$N$_2$)$_3$Mo(CO)$_3$H]$^+$[BF$_4$]$^-$

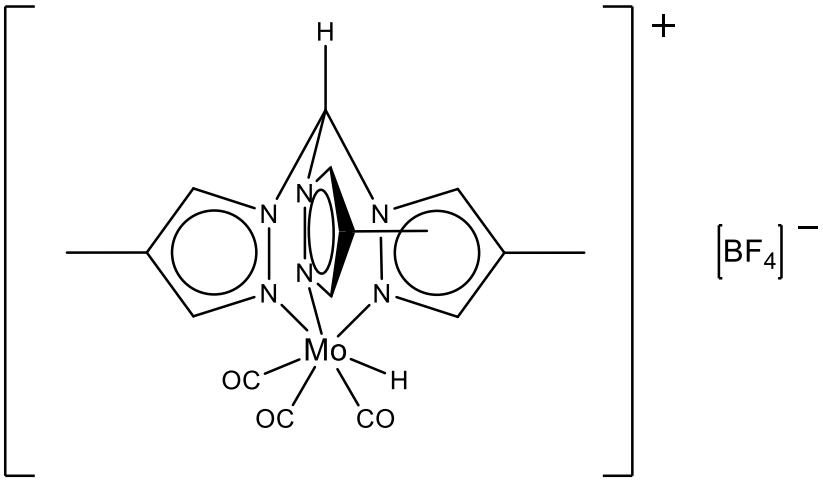

^{1}H NMR: dichloromethane-d$_2$

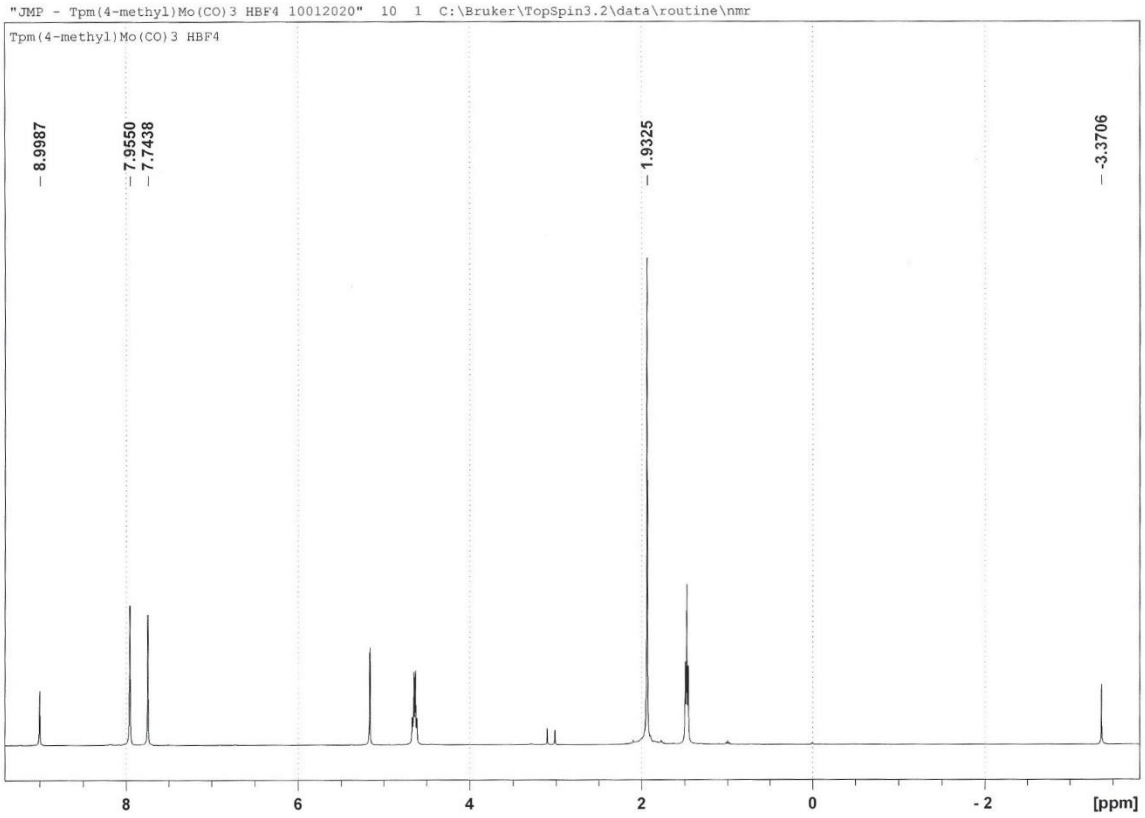

[Tpm(4-methyl)Mo(CO)$_3$I]$^+$ [I]$^-$: [HC(C$_4$H$_5$N$_2$)$_3$Mo(CO)$_3$I]$^+$[I]$^-$

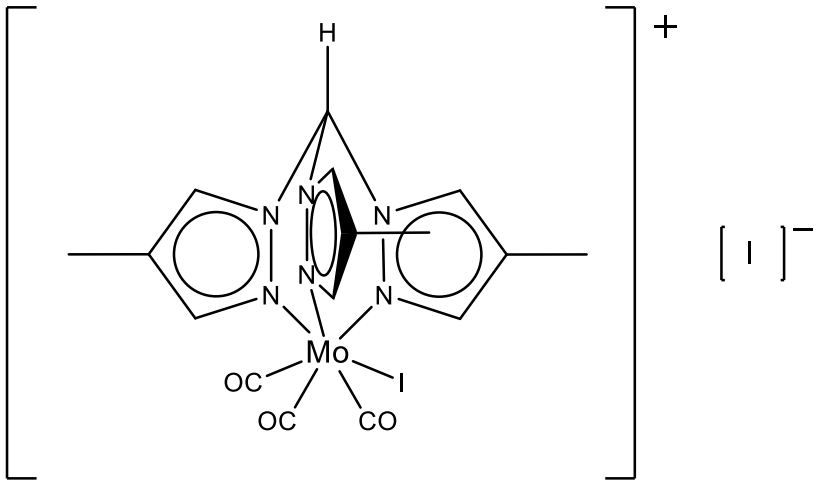

^{1}H NMR: dichloromethane-d$_2$

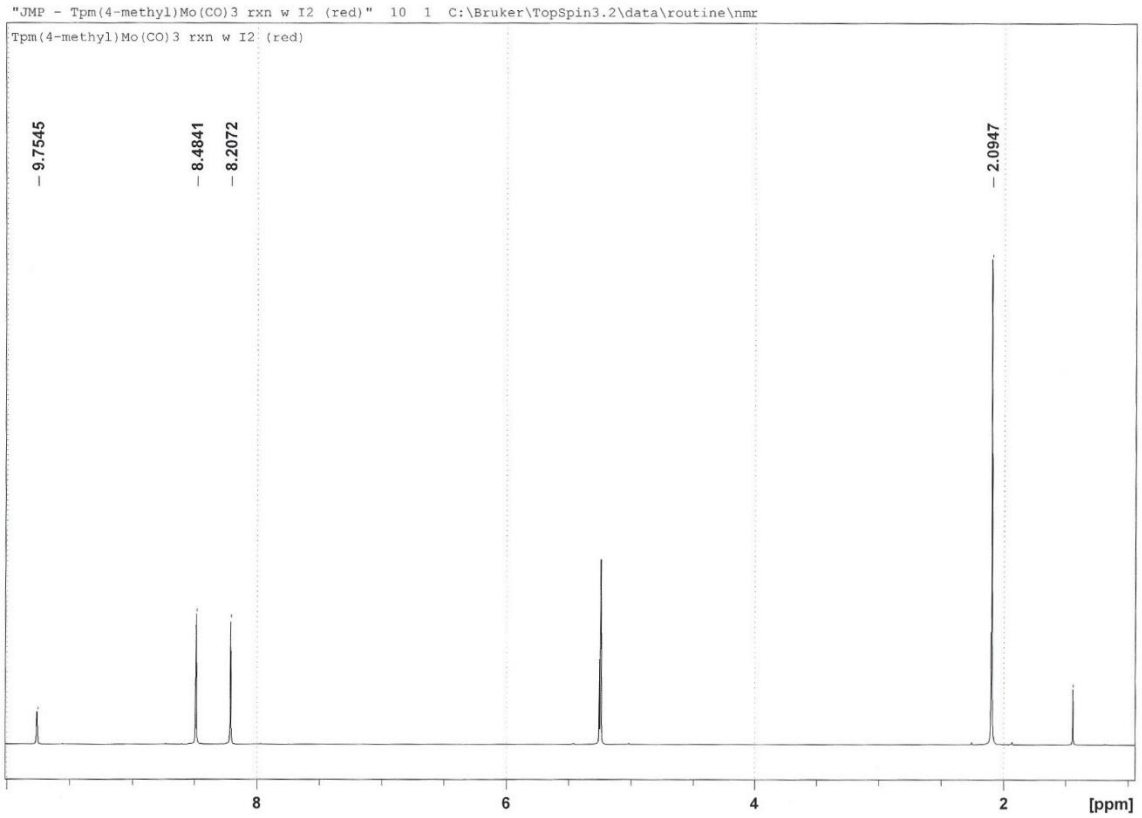

^{13}C NMR: dichloromethane-d_2

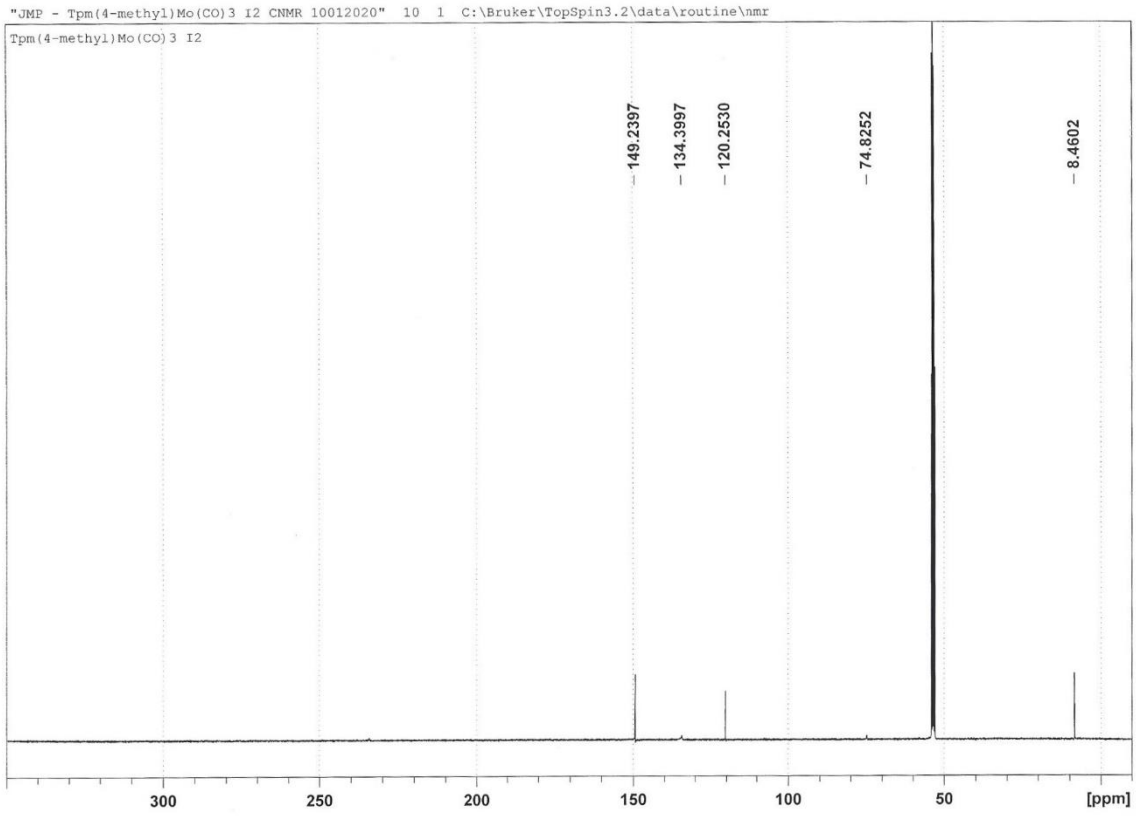

[Tpm(4-methyl)Mo(CO)$_3$Br]$^+$ [Br]$^-$: [HC(C$_4$H$_5$N$_2$)$_3$Mo(CO)$_3$Br]$^+$[Br]$^-$

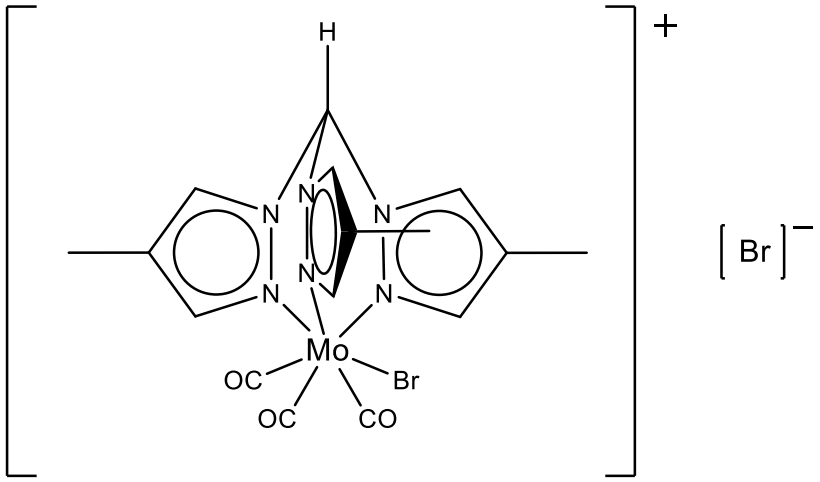

No NMR data obtained; was not successfully isolated.

IR: dichloromethane

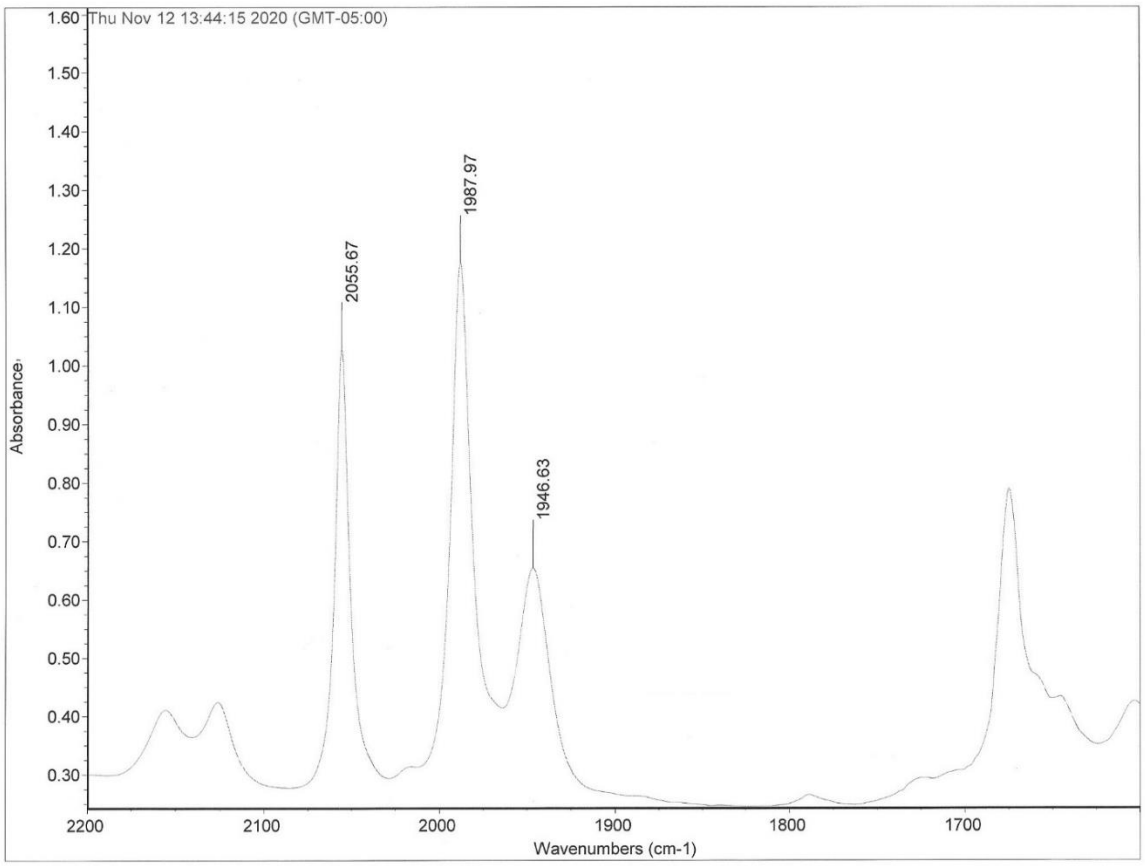

IR: dichloromethane

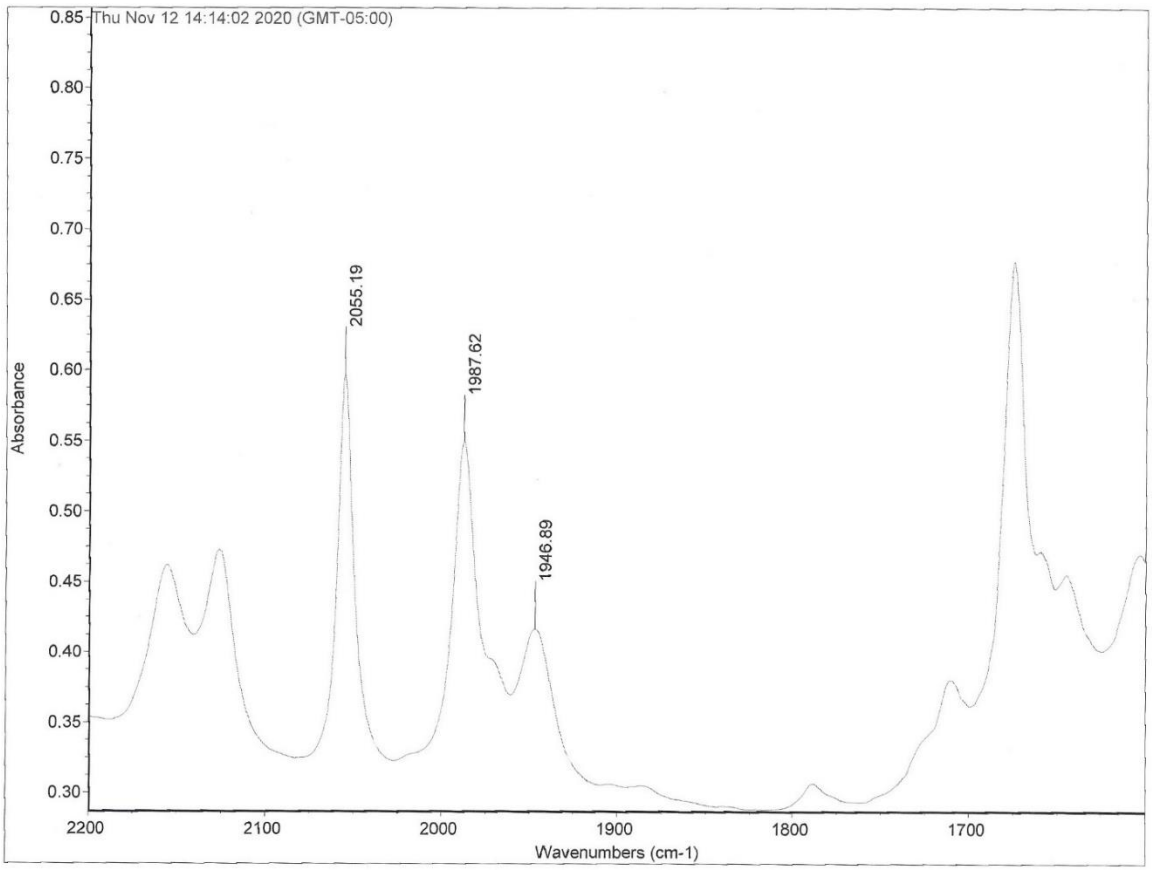

Tris(5-methyl-1-pyrazolyl)methane: $HC(C_4H_5N_2)_3$

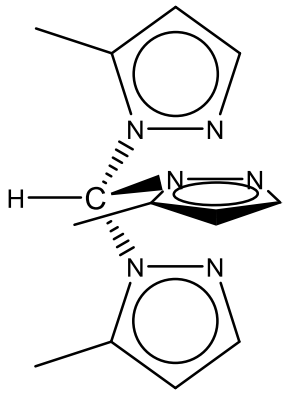

^{1}H NMR: chloroform-d_2

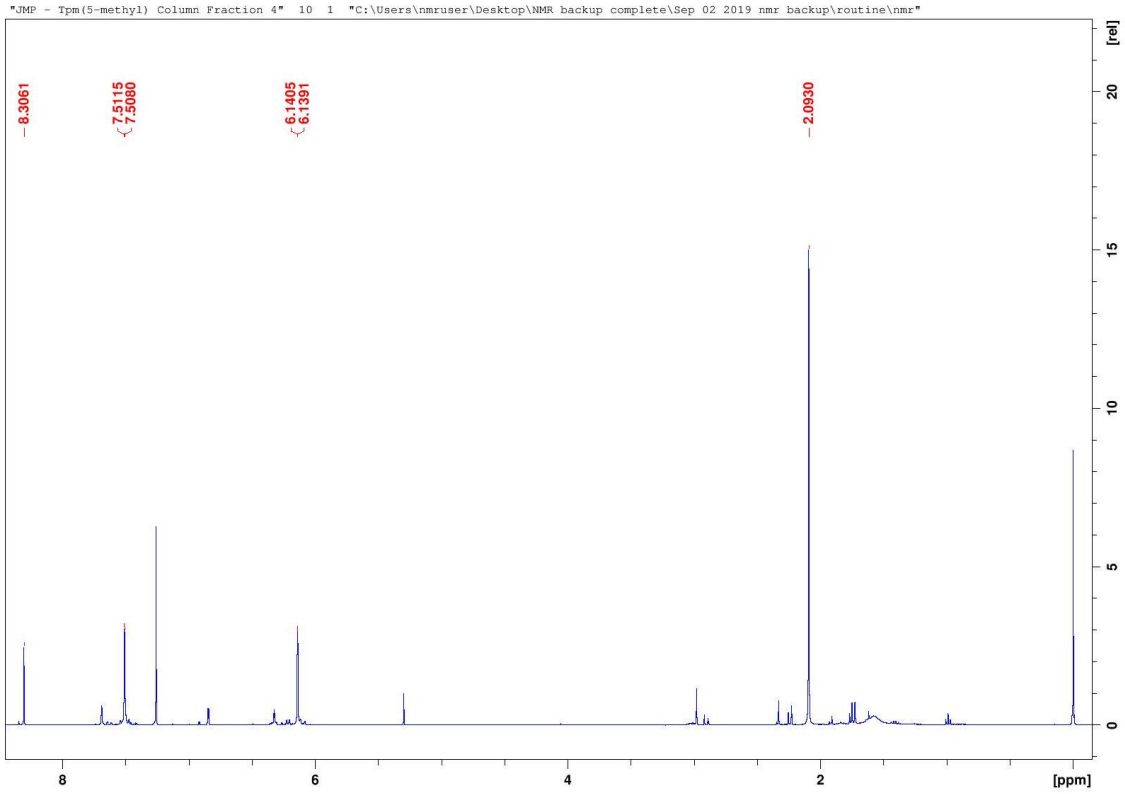

Tris(3-methyl-1-pyrazolyl)methane: $HC(C_4H_5N_2)_3$

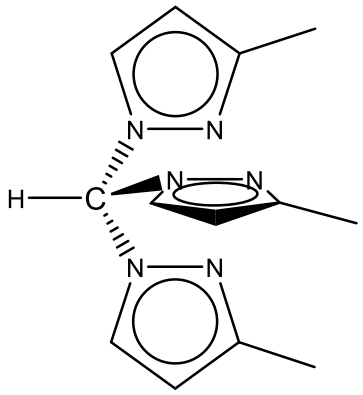

^{1}H NMR: chloroform-d

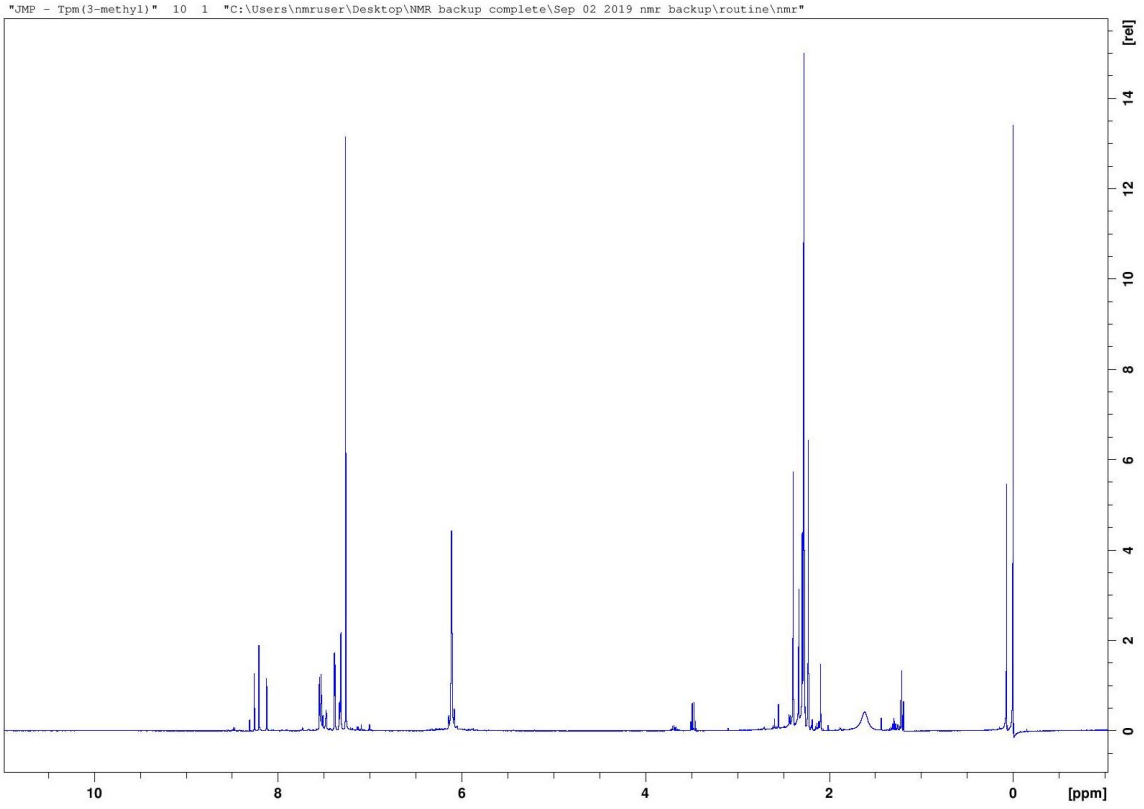

Table 2: IR Wavenumbers for CO ligands in the Various Metal Complexes. All reported values were determined in dichloromethane. Values for $[TpmW(CO)_3L]^+[X]^-$ and $[TpmMo(CO)_3L]^+[X]^-$ were observed by Dilsky.[8]

Coordination Complexes				
	Stretch 1	Stretch 2	Stretch 3	Average
$[TpmW(CO)_3L]^+[X]^-$				
$[H]^+[BF_4^-]$	2023	1938	1913	1958.0
$[I]^+[I_3^-]$	2037	1962	1930	1976.3
$[Br]^+[Br^-]$	2046	1967	1926	1979.7
$[TpmMo(CO)_3L]^+[X]^-$				
$[H]^+[BF_4]^-$	2030	1947	1926	1967.7
$[I]^+[I]^-$	2046	1980	1947	1991.0
$[Br]^+[Br]^-$	2057	1989	1948	1998.0
$[Tpm(4\text{-methyl})W(CO)_3L]^+[X]^-$				
$[H]^+[BF_4]^-$	2020	1932	1911	1954.3
$[I]^+[I]^-$	2035	1959	1926	1973.3
$[Br]^+[Br]^-$	2044	1966	1925	1978.3
$[Tpm(4\text{-methyl})Mo(CO)_3L]^+[X]^-$				
$[H]^+[BF_4]^-$	2028	1945	1926	1966.3
$[I]^+[I]^-$	2044	1978	1947	1989.7
$[Br]^+[Br]^-$	2056	1988	1948	1997.3
$[Tpm'W(CO)_3L]^+[X]^-$				
$[H]^+[BF_4]^-$	2013	1929	1896	1946.0
$[I]^+[I]^-$	2023	1949	1926	1966.0
$[Br]^+[Br_3]^-$	2038	1961	1931	1976.7
$[Tpm'Mo(CO)_3L]^+[X]^-$				
$[H]^+[BF_4]^-$	2021	1941	1918	1960.0
$[I]^+[I_3]^-$	2043	1979	1946	1989.3
$[Br]^+[Br]^-$	2048	1979	1953	1993.3